

Computer-based modeling of the conformation and packing properties of docosahexaenoic acid

Kenneth R. Applegate and John A. Glomset

Howard Hughes Medical Institute, Departments of Medicine and Biochemistry, and Regional Primate Research Center, University of Washington, Seattle, WA 98195

Abstract We used a molecular modeling approach to search for a conformation of docosahexaenoic acid (DHA) that might uniquely influence acyl chain packing in cell membranes. Studies of DHA models containing six *cis* double bonds and five intervening methylene groups identified two conformations of special interest. Both had nearly straight chain axes formed by methylene carbon alignment. In one, the carbons of the six double bonds projected outward from the methylene axis in two nearly perpendicular planes to form an angle iron-shaped molecule. In the other, the double-bond carbons projected outward from the axis at nearly 90°-intervals to form a helix. Studies of packed arrays of these hexaenes with or without saturated hydrocarbons showed that tight intermolecular packing arrangements were possible, particularly in the case of the angle iron-shaped molecules. The planar surfaces of two or more such molecules could be brought into contact "back to back," while the interplanar "V groove" of each molecule could come into close apposition with a saturated chain. Because a similar mixed chain packing arrangement was found also for 1,2 diacylglycerols, these results raise the possibility that DHA may, in certain circumstances, promote tight, regular acyl chain packing arrays in DHA-rich membranes. —Applegate, K. R., and J. A. Glomset. Computer-based modeling of the conformation and packing properties of docosahexaenoic acid. *J. Lipid Res.* 1986. 27: 658–680.

Supplementary key words diacylglycerol • acyl chain packing • monoene • arachidonic acid

4,7,10,13,16,19-Docosahexaenoic acid (DHA) is one of a group of fatty acids, found in animal cell membrane phospholipids, that cannot be synthesized *de novo* by animal cells (1). Animal cells form it, instead, from a plant-derived precursor, alpha linolenic acid, by adding four carbon atoms to the carboxyl end of the acyl chain and introducing three new *cis* double bonds. Once formed, DHA accumulates particularly in the phosphatidylethanolamine (PE) and phosphatidylserine (PS) of neuronal membranes (2) and in the PE, PS, and phosphatidylcholine (PC) of retinal rod outer segment membranes (3). In some species, including primates, it also accumulates in the membranes of spermatozoa (4). Special mechanisms may promote its accumulation in these membranes because its concentration in blood plasma is often quite low (5), and because in mature animals either it or its plant-

derived precursor must cross the blood-brain barrier or blood-testis barrier to gain access to most neurons or spermatozoa.

The fact that DHA accumulates in the membranes of neurons, rod outer segments, and spermatozoa raises the possibility that it may serve some special function in these membranes. In the case of neurons this is suggested also by the observation that the content of DHA in the PE of gray matter is consistently high (approximately 20 to 30 mole % of total fatty acids) in 45 different animal species, while corresponding values for the DHA of liver PE vary over a wide range (6). Also suggestive is the fact that diet-induced DHA deficiency in neonatal primates is accompanied by impaired visual function (7).

How a high content of DHA in membrane phospholipids might influence membrane function remains to be determined, though the presence of DHA might be presumed to affect intermolecular packing. In considering this possibility, one question that arises is whether the six *cis* double bonds of DHA favor a unique three-dimensional chain conformation that has special significance. This question cannot be answered at present because research has provided little direct information about the conformation of DHA in natural or artificial membranes (3, 8). It seemed to us, therefore, that additional studies of the conformation of DHA would be worthwhile, and that an initial, computer-based molecular modeling approach might yield clues concerning DHA that could suggest profitable directions for future experimentation. In the study described below we used the PROPHET computer system (9) with its associated molecular modeling programs to study conformational determinants in different-sized segments of the DHA chain. In addition, we studied the packing of individual polyunsaturated, mono-unsaturated, and/or saturated chains in groups of two or three, and examined the conformation of mixed diacylglycerols containing both saturated and polyunsaturated

Abbreviations: PE, phosphatidylethanolamine; PC, phosphatidylcholine; PS, phosphatidylserine.

fatty acid chains. We obtained results that emphasize the potential importance of the methylene-interrupted *cis* double-bond structure that is present in all naturally occurring membrane polyunsaturated fatty acids. Our results suggest further that a unique intermolecular packing arrangement may become possible when this structural element is repeated throughout the length of the fatty acyl chain.

METHODS

Molecular modeling using the PROPHET computer system

Molecular modeling and data manipulation were performed on the PDP-10 computer of the National Institutes of Health PROPHET system. PROPHET supports an integrated package of software designed for molecular modeling (10), which may be used to generate the atomic coordinates of a three-dimensional molecular model having approximately correct geometry for bond lengths and angles and torsion angles. The model can be displayed on a graphics terminal, and the display can be manipulated to show the molecule from any viewpoint. In addition, the molecular geometry can be modified by commands that rotate portions of the molecule about single bonds. Other commands allow measurement of distances and angles of interest in the model. Finally, it is possible to generate structures containing models of several molecules, and to manipulate individual molecular components with respect to one another.

The PL/PROPHET language (11), a subset of PL/I, allows users to write applications programs. A full set of molecular modeling commands is provided as part of the language.

Optimization of molecular conformations

PROPHET contains an interface to the updated 1977 version of the MM2 molecular mechanics program developed by Allinger and coworkers (12–14). The general validity of this program has been discussed (12). The interface in PROPHET performs the details of coding a standard molecular model in terms of the atom and bond classifications used by MM2, writing the MM2 input file, running the program, retrieving the MM2 output files, and setting the model to the new minimum energy conformation (15, 16). MM2 attempts to relax all the internal degrees of freedom in a molecular model, and to adjust it to a minimum steric energy conformation by non-linear least squares methods. Steric energy is defined as comprising all energy contributions (exclusive of electronic bonding energies), such as those for bond stretching, bending, and rotation, plus van der Waals forces, electrostatic, and dipole interactions. The zero point of steric

energy is defined for a fictitious molecule having all bond lengths and angles set to their nonstrained equilibrium values, and having no torsional or non-bonded interaction energies.

Two limitations of the MM2 program have affected the study reported here. First, a maximum of 100 atoms can be used in a given calculation, thus precluding the study of large arrays of molecules and requiring the use of truncated acyl chains in some models. Second, parameters for P and O atoms in phosphate are not yet available, so phospholipid head groups cannot be modeled.

Estimation of steric energies for non-equilibrium conformations

In order to permit rapid examination of the conformation-dependent variations of steric energy in a flexible molecule, a program called ENCHECK was written in the PL/PROPHET language. ENCHECK steps through a set of conformations and evaluates the variable component of the steric energy for each one. It permits specification of a set of single bonds to be rotated in the model. For each bond, the range of dihedral angles and operating mode (random twists, random selection from a fixed set of dihedral angles, or sequential stepping over a set of dihedral angles) may be specified. The molecular segments between the rotated bonds are treated as rigid structures. However, an initial calculation computes the internal van der Waals energy of these segments, which is thereafter added to the variable torsional and van der Waals parts of the steric energy. ENCHECK uses the same parameters and functions for the torsional and van der Waals energies that are employed in MM2 (14).

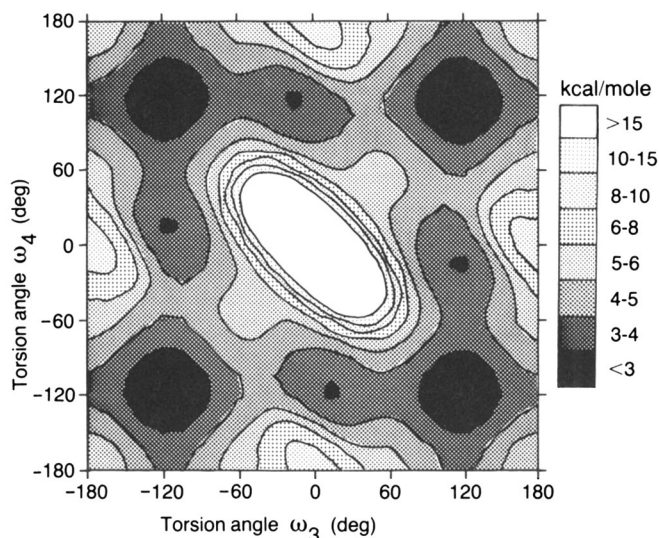
Torsion angle conventions

All torsion angles (ω) for bond rotation in the computer models are designated according to the conventions of Sundaralingam (17) and Hauser et al. (18). They are defined in terms of the principal non-hydrogen substituent atoms attached to the atoms that form the bond. The 0° reference angle corresponds to overlapping, or eclipsed principal substituents as viewed along the bond axis (see, for example, Fig. 3 in Hauser et al. (18)). Positive angles correspond to clockwise rotations at the far end of the bond. We adopt the commonly used nomenclature of *cis* ($\omega = 0^\circ$), *gauche* ($\omega = 60^\circ$), *skew* ($\omega = 120^\circ$), and *trans* ($\omega = 180^\circ$), though one of the references cited (19) employs a notation in which the *trans* conformation is assigned an angle of 0° while *cis* is set at 180°.

Contour maps of steric energy for 1,4-pentadiene and n-pentane

Maps of steric energy versus the torsion angles ω_3 and ω_4 about the central carbon atom 3 in each molecule of 1,4-pentadiene or n-pentane (Fig. 1) were generated as

A. STERIC ENERGY OF 1,4-PENTADIENE



B. STERIC ENERGY OF N-PENTANE

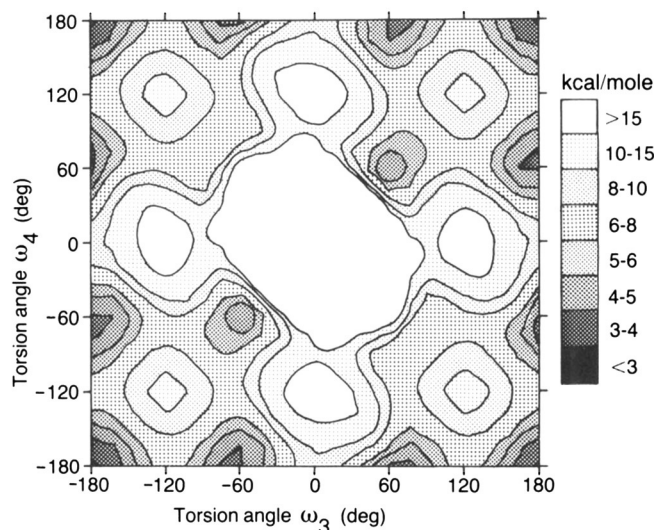


Fig. 1. Steric energy maps contrasting (A) 1,4-pentadiene with (B) n-pentane. The maps were generated as described in Methods. The MM2 molecular mechanics program was first used to optimize the molecules at all their distinct local energy minima (Table 1). Program ENCHECK then varied central torsion angles ω_3 and ω_4 (as defined in Table 1) in 10-degree increments over restricted ranges centered on the various minima. Data for these subranges were then combined, and the PROPHET program CONTOUR was called to produce the energy maps. Energy ranges in kcal/mole are shown by shaded contour levels. For B, note that the lowest energy values (<3 kcal/mole) correspond to shaded areas that are so narrow that they are barely visible at the extreme corners of the figure.

follows. Local minimum-energy molecular conformations identified by MM2 were used as the starting point for ENCHECK calculations of steric energy over a range of neighboring nonequilibrium conformations. This allowed a more accurate representation of the internal bond lengths and angles in each neighborhood than an averaged

geometry would have provided. Energies for conformations lying on the boundaries between two or more such regions were found to vary by as much as 0.5 kcal depending on the starting conformation used. These values were averaged using a weighting procedure as follows. Weighting factors were calculated as the inverse square of the vector distance $[\Delta\phi, \Delta\psi]$ between that conformation and the local minimum-energy conformation used to generate it. This weighting method produced smooth joins between the regions. Together with appropriate symmetry considerations, it allowed the construction of steric energy contour maps such as shown in Fig. 1 to an accuracy of a few tenths of a kcal per mole over the entire 360° ranges of ω_3 and ω_4 torsion angles. The maps were generated with the public program CONTOUR available in PROPHET (20).

Initial surveys of intermolecular packing interactions

Another PL/PROPHET program, EMAPMM, was written to allow rapid calculation of the intermolecular van der Waals energy for a large number of relative orientations of two molecules. EMAPMM allows the user to define various sequences of translation and rotation of the two molecules with respect to one another. The energy of interaction is computed for each step in the sequence. Each molecule is assumed to have a rigid conformation, and its internal steric energy is omitted from the calculation. EMAPMM uses the same van der Waals energy functions and parameters as MM2 does (14). The energy curves of Fig. 7 were calculated with EMAPMM.

Calculation of packing energies

Packed arrays of hydrocarbons were created by combining models of MM2-optimized individual components in a PROPHET multimolecule structure. After the components were positioned in the desired starting orientations, coordinates were transferred to a disjoint pseudo-molecular structure that could be submitted to MM2 for further optimization. For packings of two molecules, 19-carbon hexaenes ($\Delta 1, 4, 7, 10, 13, 16$), 16-carbon saturated chains, and 16-carbon monoenes ($\Delta 9$) were used. For packings of three molecules, the chains were truncated to 13-carbon tetraenes ($\Delta 1, 4, 7, 10$), 10-carbon saturated chains, and 11-carbon monoenes ($\Delta 5$). Raw packing energies were calculated as the difference between MM2 steric energies for the packed array and the separate components. Studies had shown that MM2 energies were a linear function of chain length for single saturated chains, polyunsaturated angle iron conformations, and combinations of these in arrays of two packed molecules. Thus, it seemed justified for purposes of comparison to perform a linear extrapolation of all packing energies to the energy expected if all chains had a common length of 20 Å. Finally, optimum packing energies were quite similar if expressed as average energy per pair-wise molecular interaction. This latter

quantity was approximated by dividing the normalized packing energy by $(m - 1)$ where m was the number of packed molecules.

Space-filling views of molecules

Program SPMOL, an updated version of existing PROPHET public program (21), was used to generate views of molecules similar to those that could be constructed from Corey-Pauling-Koltun (CPK) models. MM2 van der Waals radii were used (14), and methods of input were devised to allow SPMOL to recognize MM2 atom classifications.

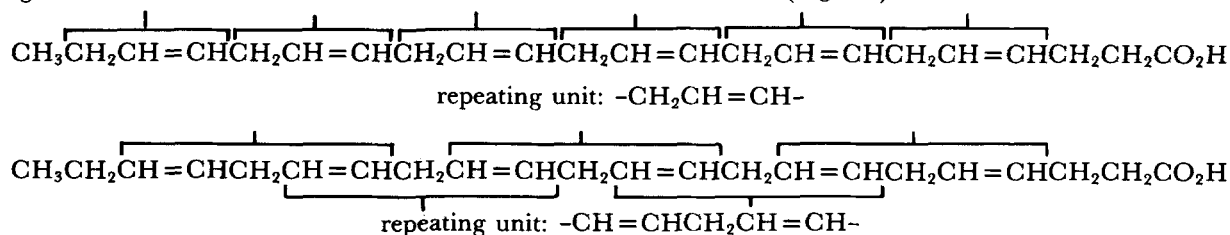
Molecular cross-sectional areas

PL/PROPHET program MOLXSECTION was written to allow calculation of cross-sectional areas of molecules. A numerical integration of the area was accomplished by finding the intersections of a test vector with the atoms as the vector was moved in small steps across the molecule in the plane of the cross section. At each step, the total length of the vector contained within atoms of the molecule was multiplied by the transverse step size and added to the total area. A step size of 0.05 \AA was adequate to yield cross-sectional areas in \AA^2 accurate to two decimal places. Cross-sectional areas could be calculated either for thin slices through the molecule or for projections of the entire molecule onto an arbitrary plane. MM2 van der Waals radii were used in all calculations (14).

RESULTS

Studies of propene and 1,4-pentadiene

In DHA, as in other polyunsaturated fatty acids, pairs of adjacent *cis* double bonds are separated from one another by a single methylene carbon. DHA is unusual, however, because its six double bonds and five intervening methylene carbons form a regular structure that extends through most of the acyl chain. This structure can be visualized as a succession of directly linked, propene-like segments or as a sequence of overlapping, 1,4-pentadiene-like segments:



In initial molecular modeling studies we therefore focused attention on these segments in an effort to identify determinants that might affect the conformation of the complete DHA chain.

We constructed models of propene and 1,4-pentadiene, then used MM2 to refine the models and identify low-energy conformations. The MM2 refinements agreed with published experimental studies (19, 22–25) and modeling studies (19, 26, 27) in predicting that the torsion angle for a carbon-carbon single bond adjacent to a double bond is $\pm 118^\circ$, i.e., close to the *skew* (120°) conformation rather than the *gauche* (60°) or *trans* (180°) conformation (results shown for 1,4-pentadiene in Table 1). In contrast, an MM2 refinement of n-pentane, done for comparison, yielded torsion angle values that were very close to the *trans* conformation (Table 1). A contour map of energy versus the two torsion angles for the carbon-carbon single bonds in 1,4-pentadiene revealed that the minima centered on the *skew* conformations were rather broad (Fig. 1A). These minima contrasted sharply with the very localized minima at the *gauche* and *trans* conformations of n-pentane (Fig. 1B). Furthermore, torsional energy barriers along pathways between conformations were 2 to 3 kcal lower in 1,4-pentadiene than they were in n-pentane.

The minimum energy conformations obtained for 1,4-pentadiene were of special interest for geometric reasons. When *both* carbon-carbon single bonds were rotated in the same direction by either $+118^\circ$ or -118° , the double bond planes were positioned essentially at a right angle with respect to one another, and the double-bond directions were parallel (Fig. 2A). This conformation was unique. It was possible to generate a continuous series of paired bond rotations about the methylene carbon that yielded perpendicular double-bond planes (Fig. 3). Within the series, however, the double-bond directions were aligned in parallel *only* for paired rotations of $+118^\circ$ with $+118^\circ$ (*skew+*, *skew+*) or -118° with -118° (*skew-*, *skew-*).

A conformation that had similarly low energy but a very different shape was obtained when one carbon-carbon single bond in 1,4-pentadiene was rotated by $+118^\circ$ and its neighbor was rotated by -118° , i.e., in the *opposite* direction. In this *skew+*, *skew-* conformation the double-bond planes intersected at a dihedral angle of 120° , and the double-bond *directions* were nearly perpendicular to one another (Fig. 2B).

Because the results obtained for these two low-energy conformations generally agreed with published data obtained by direct experimentation and by modeling (Table 2), they provided a measure of the validity of the molecu-

TABLE 1. Geometry and steric energies for conformations of 1,4-pentadiene and n-pentane optimized by MM2

Molecular Parameters	1,4-Pentadiene Conformers			n-Pentane Conformers			
	Skew + Skew +	Skew + Skew -	Skew + Cis	Trans Trans	Trans Gauche +	Gauche + Gauche +	Gauche + Gauche -
Torsion angles (degrees)							
ω_2	.04	.05	.11	179.83	179.46	174.69	169.68
ω_3	117.83	118.00	114.79	179.93	175.41	60.03	79.55
ω_4	118.13	-118.30	-11.55	179.87	64.78	60.01	-77.78
ω_5	.04	-.04	.54	179.99	174.62	174.71	-169.08
Steric energy terms (kcal/mole)							
Bond bending and stretching	.39	.35	.79	.68	1.02	1.47	2.20
Torsional	.10	.12	.29	.01	.46	.80	1.62
Van der Waals non-bonded	1.51	1.60	1.82	2.13	2.24	2.58	2.58
Total steric energy	2.00	2.07	2.90	2.82	3.72	4.86	6.40
Contribution to equilibrium mixture (percent) ^a							
	43 ±	38 ±	19 ±	50 ±	44 ±	6 ±	0.2 ±

Designations of the conformers shown in the table are based on the torsion angle conventions described in Methods. Torsion angles ω_2 , ω_3 , ω_4 , ω_5 follow the subscript notation of Go and Scheraga (35): ω_2 is defined by atoms H-C₁-C₂-C₃, ω_3 by C₁-C₂-C₃-C₄, ω_4 by C₂-C₃-C₄-C₅, and ω_5 by C₃-C₄-C₅-H.

^aComputed from the Boltzmann probability factor: $P_i = w_i \exp(-E_i/kT) / \sum w_i \exp(E_i/kT)$ where E_i is the steric energy of a given conformation, R = gas constant = 1.9872×10^{-3} kcal/mole-degree K, T = absolute temperature, assumed = 273°K, and w_i is the weighting factor for the number of degenerate conformations.

lar modeling programs used. Furthermore, they emphasized the importance of the 1,4-pentadiene-like structure as a determinant of the conformation of polyunsaturated fatty acids, and showed, in particular, that multiple *cis* double bonds in a polyenoic fatty acid need not cause sharp axial bends in the main chain axis.

Conformations of a 19-carbon, hexaenoic hydrocarbon chain

To determine how a sequence of 1,4-pentadiene-like segments might affect the conformation of a hexaenoic molecule such as DHA, we generated a 19-carbon model of DHA that lacked the carboxyl group and the two succeeding methylenes of the fatty acid, but included both the polyunsaturated portion and the terminal ethyl group. In this hydrocarbon the five methylene carbons that individually separated the six *cis* double bonds all initially had torsion angles of +118°, whereas the two terminal carbon-carbon bonds had torsion angles of -90° and 180°. MM2 computations for small polyunsaturated molecules containing terminal alkyl groups had revealed that a terminal ethyl group that immediately follows a typical polyenoic sequence of double bonds uniquely shows an optimum sequence of torsion angles corresponding to ± 90° and 180° (data not shown). Longer terminal alkyl chains showed the ± 120° skew angle, followed by 180° *trans* angles.

We used the ENCHECK program to set systematically each of the 10 torsion angles associated with the five intervening methylenes at either +118° or -118°, while keeping constant the torsion angles associated with the two terminal carbons. ENCHECK generated all 1024 possible conformations and computed the combined torsional and van der Waals energies for each one.

The energy distribution of about 70% of the conformations fell within the relatively narrow range of 24.5 to 36 kcal/mol as shown in Fig. 4, while the energies of the remaining conformations ranged from 36 to 13,800 kcal. Those conformations at the very low end of the energy spectrum showed a "hairpin" bend in the hydrocarbon chain that favored van der Waals associations between hydrogen atoms at the opposite ends of the chain (see Fig. 5). The "hairpin" bend was caused by torsion angle sequences such as -118°, +118° and +118°, -118° at two successive methylene carbons, where -118°, +118° and +118°, -118° each refer to torsion angles at two single, carbon-carbon bonds involving a central methylene carbon. Refinement of the lowest energy "hairpin" by MM2 led only to a slight change in the conformation (not shown), but decreased the steric energy by about 13.2 kcal. A similar "hairpin"-shaped conformation was found in a computer modeling study of arachidonic acid (28).

Conformations whose energy fell approximately within the range of 25 to 27 kcal/mole also had bent hydrocarbon chains (not shown), which were associated with torsion angle sequences of +118°, -118° and/or -118°, +118°. In contrast, conformations of only slightly higher energy had extended hydrocarbon chains and torsion angle sequences of only +118°, +118° and/or -118°, -118°. When all ten torsion angles had the same sign, the result was a helical conformation such as that indicated by one of the arrows in Fig. 4 and shown in detail in Fig. 6A. The five methylene carbon atoms intervening between the double bonds defined a straight central axis. The double bonds were parallel to the axis, while successive double-bond planes containing the axis were rotated by 90° steps and formed a helix about the axis. Because the repeat length of the helix corresponded to four double bonds, the

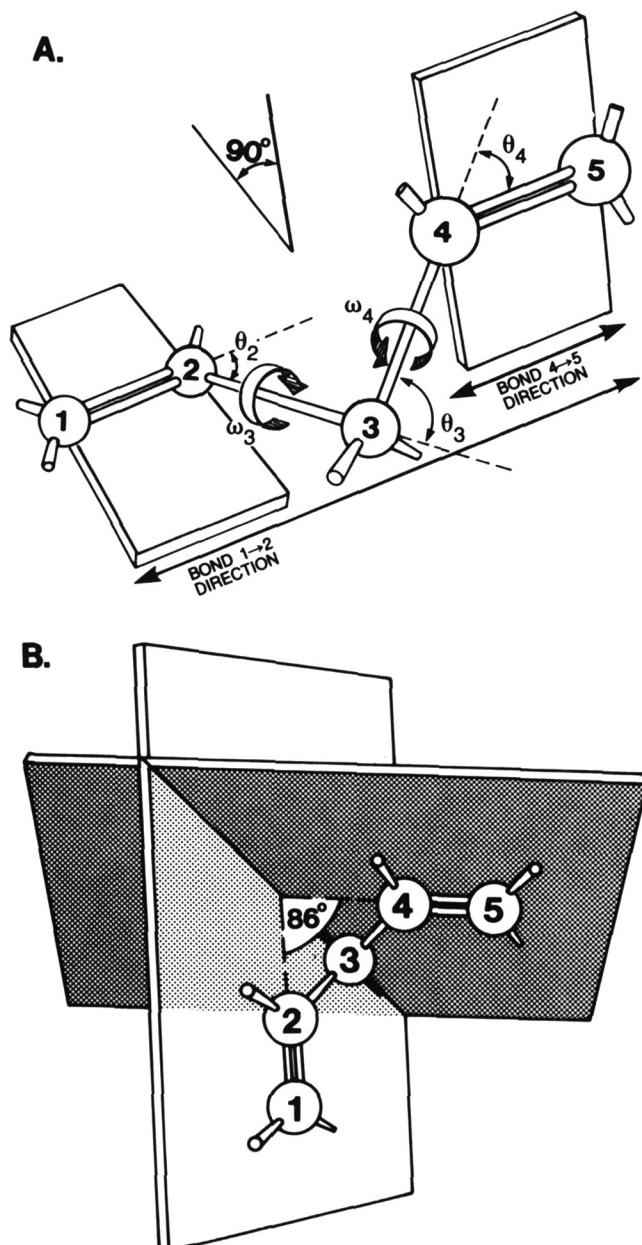


Fig. 2. Spatial orientation of double bond planes and double bond directions in stable conformations of 1,4-pentadiene. A. The *skew, skew* form, characterized by values of $+118^\circ, +118^\circ$ or $-118^\circ, -118^\circ$ for torsion angles ω_3 and ω_4 about the central methylene (see Methods and Table 1 for torsion angle conventions). Bond and torsion angles are defined according to the notation of Go and Scheraga (35). Each θ_i refers to 180° minus the C-C-C bond angle at atom i , while each ω_i is the torsion angle about the bond between atoms $i-1$ and i . Bond angle supplements determined for MM2 minimized models are $\theta_2 = \theta_4 = 180^\circ - 123.9^\circ$, $\theta_3 = 180^\circ - 110.0^\circ$. Also, carbon-carbon bond lengths are 1.32 Å for double bonds and 1.54 Å for single bonds. B. The *skew+, skew-* form (values of $+118^\circ, -118^\circ$ for torsion angles ω_3 and ω_4).

planes of double bonds 1 and 5 were essentially aligned as were those of double bonds 2 and 6. The steric energy of the helix, calculated by ENCHECK, was about 3 kcal/mole higher than that of the "hairpin shaped" conformation shown in Fig. 5. Refinement of the helix by MM2

decreased the steric energy by 12.6 kcal and also decreased the helical pitch. Because all ten torsion angles decreased to 104° , the repeat length of the helix decreased to 3.3 double bonds, and double bonds 1 and 4 became roughly coplanar as did double bonds 2 and 5 (not shown). Helical conformations of DHA have been postulated by Stubbs and Smith (8) and by Dratz and Deese (3).

Another type of extended conformation, also indicated by an arrow in Fig. 4, was shaped like an angle iron (Fig. 6B). It was generated when pairs of 118° torsion angles associated with successive intervening methylene carbons showed the following alternating sequence or its mirror image: $+118^\circ, +118^\circ$; $-118^\circ, -118^\circ$; $+118^\circ, +118^\circ$; $-118^\circ, -118^\circ$, $+118^\circ, +118^\circ$. As in the case of the helical conformation, the five intervening methylene carbons defined a straight-chain axis and the double bonds were parallel to it. However, successive double-bond planes projected outward from the axis in two, rather than in four, different directions. Double bonds 1, 3, and 5 formed one plane, while double bonds 2, 4, and 6 formed a second plane perpendicular to the first. This "angle iron-shaped" conformation was a simple extension of the conformation of 1,4-pentadiene shown in Fig. 2A, and had a total steric energy very close to that of the helical conformation. Refinement of the angle iron-shaped hexaene by MM2 decreased the steric energy by 12.1 kcal and led to a slight curve in the methylene axis (not shown). Based on the crystal structure of linoleic acid, Ernst, Sheldrick, and

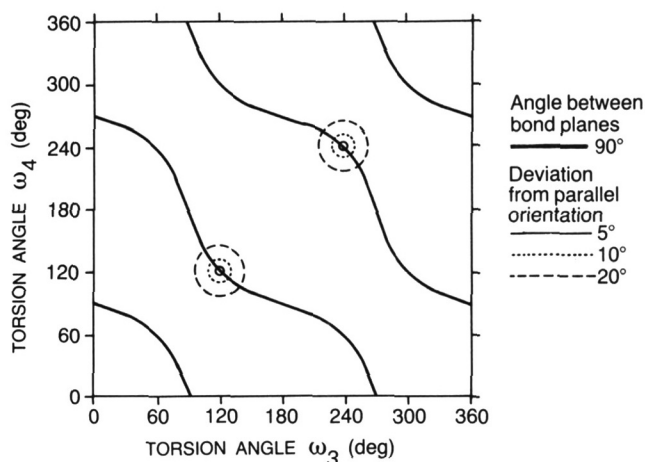


Fig. 3. Unique geometric criteria defining an extended conformation of 1,4-pentadiene. Simultaneous solution of equations for α , the dihedral angle between double-bond planes, and β , the angle between double-bond vectors as functions of torsion angles ω_3 and ω_4 . (See Appendix I for development of the equations from the formalism of Go and Scheraga (35).) The sinusoidal lines indicate pairs of torsion angles about the methylene group that yield a 90° dihedral angle between double-bond planes. The circular regions surround the two torsion angles that uniquely yield parallel double-bond vectors (see Fig. 2A). These torsion angles, $\omega_3 = \omega_4 = +118^\circ$ or -118° , as indicated by the exact intersection of the sinusoidal curves with the center of the circular regions, agree closely with the MM2 minimum energy conformations presented in Table 1.

TABLE 2. Steric energies of 1,4-pentadiene obtained in the present study and two other studies

Conformer	Steric Energy		
	This Study ^a	Gallinella and Cadioli ^b	Schurinck and de Jong ^c
	kcal/mole		
1. <i>Skew</i> +, <i>skew</i> +	2.00	2.00	2.00
2. <i>Skew</i> +, <i>skew</i> -	2.07	1.86	2.21
3. <i>Skew</i> +, <i>cis</i> (-)	2.90	1.58	
4. <i>Skew</i> +, <i>gauche</i> +	3.88	4.62	5.34
5. <i>Skew</i> +, <i>gauche</i> -	3.43	3.42	4.96
6. <i>Skew</i> +, <i>trans</i>	3.64	3.82	5.02
7. <i>Trans</i> , <i>trans</i>	6.10	5.33	6.67
8. <i>Gauche</i> +, <i>gauche</i> +	5.30	7.90	8.31
9. <i>Gauche</i> +, <i>gauche</i> -	8.60	13.47	9.26
10. <i>Gauche</i> +, <i>trans</i>	5.50	5.39	7.32
11. <i>Cis</i> , <i>gauche</i> +	5.80		
12. <i>Cis</i> , <i>trans</i>	10.00	10.15	
13. <i>Cis</i> , <i>cis</i>	223.00		

Values reported by other workers were recalculated in units of kcal/mole if necessary, and rescaled so that the energies for the most stable *skew*, *skew* conformer coincided at 2.0 kcal/mole. Note that the other studies employed fixed bond lengths and angles in a rigid geometry for their quantum mechanical calculation, whereas MM2 permitted these parameters to vary.

^aRelative to hypothetical unstrained state with no non-bonded interactions.

^bData from reference 19.

^cData from reference 27.

Fuhrhop (25) postulated an angle iron-shaped conformation for the polyenoic segments of linolenic and arachidonic acids.

Additional extended conformations (not shown), in which segments of helix and angle iron were combined, had energies close to those of the homogeneous extended conformations. In contrast, conformations at the very high end of the energy spectrum, i.e., >50 kcal/mole, were characterized by bends that caused intramolecular collisions. The bends in these cases were created by torsion angle sequences of $+118^\circ$, -118° or -118° , $+118^\circ$ at multiple methylene carbons. The highest energy conformation consisted entirely of these sequences.

Our studies of isolated hexaenoic hydrocarbon chains thus identified several potentially interesting conformations. The hairpin-shaped conformations seemed of interest because they had the lowest total steric energy. This raised the possibility that isolated molecules of DHA might tend to be hairpin-shaped. The two homogeneous extended conformations were of special interest because it seemed likely that they would be favored in condensed monolayers and bilayers. We therefore focussed attention on them in a series of studies of the packing properties of hexaenoic hydrocarbon chains.

Interchain packing of angle iron-shaped hexaenes

To examine the packing of the extended hexaenes we first performed detailed studies of model, angle iron-shaped polyenes in which we sought to identify preferred

packing arrangements for groups of two or three such molecules. In addition, because neuronal phospholipids that contain a DHA chain typically also contain a saturated chain, we studied the interactions of angle iron-shaped polyenes with saturated molecules. EMAPMM identified packing arrangements of low intermolecular van der Waals energy that could be used as starting points for refinement by the MM2 program. Fig. 7A defines the coordinate system for a typical EMAPMM survey using two 17-carbon hexaenoic hydrocarbons in the angle-iron conformation. Figs. 7B-7D show the intermolecular energy variations for successive one-dimensional traverses parallel to the three coordinate axes in the neighborhood of one local minimum energy position (corresponding to Fig. 7A). Similar traverses or energy evaluations on a Cartesian grid pattern helped to identify other low-energy regions, as did search patterns involving rotation or radial motion of one molecule about a second molecule, or rotation of a molecule about its own axes.

Two low-energy packings for identical angle iron-shaped hexaenes so identified formed the basis for the MM2 refinements shown in Fig. 8. Note that 19-carbon hexaenes

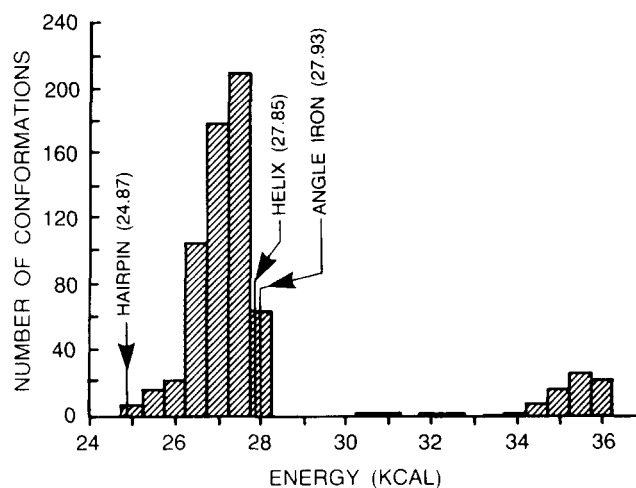


Fig. 4. Energy distribution for conformations of an isolated, 19 carbon hexaene. A computer model of all *cis* $\text{CH}_2=\text{CH}-\text{CH}_2(\text{CH}=\text{CHCH}_2)_3\text{CH}_2\text{CH}_3$ was constructed based on the MM2 minimum energy geometries found for the *skew* +, *skew* + and *skew* +, *skew* - conformations of 1,4-pentadiene (Fig. 2; Table 1). Bond lengths and angles that had been found for the two 1,4-pentadiene conformations were averaged, particularly to remove asymmetries involving the methylene carbons. The average values were then used to construct a hybrid hexaene that would not favor one combination of 118° torsion angles over another. The terminal ethyl group of the hexaene was modeled from the MM2 geometry obtained for 1,4-heptadiene. The ENCHECK program was used to generate all possible combinations of $+118^\circ$ or -118° torsion angles at the ten, single carbon-carbon bonds separating the six double bonds. The histogram shows the distribution of the sum of van der Waals and torsional conformational energies for the lower 70% of the conformations. The low energy "hairpin" conformation of Fig. 5 and the extended "angle iron" and helical conformations of Fig. 6 are indicated specifically.

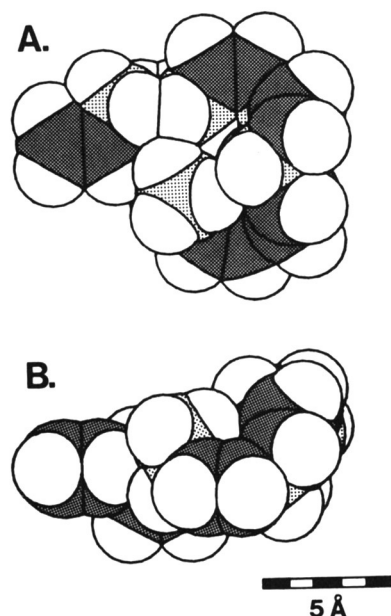


Fig. 5. The "hairpin" conformation of lowest energy for an isolated hexaenoic hydrocarbon, as determined by the ENCHECK calculations used to generate the histogram of Fig. 4. The sequence of signs for the 118° torsion angle rotations was $--, --, -, +, --, --$. The conformation was refined subsequently using MM2. In it, as in other "hairpin" conformations, a $skew+, skew-, skew-, skew+$ sequence of double bonds creates two 90° bends (see Fig. 3B) which together cause the chain to fold back on itself. A. View showing full "hairpin" bend. B. Side view. C- sp^2 carbons of the double bonds are indicated by dark shading, other carbons by light shading. Hydrogens are unshaded.

were used for these refinements to include the two saturated carbons at the DHA chain terminus. In the first packing arrangement (Fig. 8A), one angle iron-shaped hexaene was rotated by 180° with respect to the second one and paired "back-to-back" with it so that opposing planes of double bonds made contact. The side view shows that double bonds 1, 3 and 5 from each of the contacting planes were aligned with one another, as would be predicted from the identified minimum shown in Fig. 7D. The double-bond carbons that contributed to the contacting planes were oriented in opposite directions in an "anti-parallel" arrangement, which prevented steric interference between the methylene hydrogens of the two hexaenes and allowed the methylene hydrogens of one hexaene to interact favorably with the hydrogens of the double-bond carbons of the other hexaene. The energy and cross-sectional area calculated for this refined packing arrangement are shown in Fig. 9, packing 1.

The "stairstep" packing arrangement of three angle iron-shaped tetraenes shown in Fig. 10A is a simple extension of the "back-to-back" packing arrangement in Fig. 8A. Data for this packing arrangement are shown in Fig. 9, packing 4. Note that the packing energy per interacting pair of molecules, scaled for a common length of 20 Å, remained in the same range of -12 to

-13.5 kcal when the number of polyenes was increased from two to three.

In the second low-energy packing arrangement of two identical angle iron-shaped hexaenes, identified by the approach shown in Fig. 7, the interplanar "V grooves" of the two hexaenes faced one another, and the opposing double bonds were interleaved (Fig. 8B). In this "edge-to-edge" packing arrangement, the double bond hydrogens of the two polyenes came into close apposition. The energy and cross-sectional area values (Fig. 9, packing 2) were similar to those obtained for the "back-to-back" packing arrangement. Both arrangements were very compact and involved little conformational distortion.

Somewhat less effective packing occurred in other arrangements, such as one (Fig. 9, packing 3) in which the double-bond planes of two identical angle iron-shaped hexaenes were aligned "back-to-back," but with the double-bond carbons oriented in the same direction. In this case steric interference between methylene hydrogens on the two molecules was associated with a packing energy of only -11.9 kcal, about 1 kcal higher than the values for the two optimum conformations.

Less effective packing also occurred between angle iron-shaped hexaenes that were mirror images of one another (not shown). Two such hexaenes could be aligned "back-to-back" in a packing arrangement analogous to that shown in Fig. 9, packing 1 to yield a cross-sectional area of 28.35 \AA^2 per molecule. However, the packing energy was -11.39 kcal/mole as compared with -13.19 kcal/mole for the arrangement of identical hexaenes. Two angle iron-shaped hexaenes that were mirror images could also be aligned in an "edge-to-edge" arrangement analogous to that shown in Fig. 9, packing 2. However, interleaving of the double bonds of the two molecules was not possible because the opposing double bonds occupied comparable positions in each chain. The cross-sectional area was therefore larger than that of paired identical hexaenes (26.90 \AA^2 per molecule as compared with 25.77 \AA^2 per molecule), and the packing energy was higher (-11.49 kcal/mole as compared with -12.88 kcal/mole).

When we studied the interaction of angle iron-shaped hexaenes with saturated hydrocarbons, we found again that compact, low-energy packing was possible with minimal distortion. Two low-energy packing arrangements could be identified for an angle iron-shaped 19-carbon hexaene and an all-*trans*, 16-carbon saturated chain. In one (Fig. 9, packing 5), the broad side of the saturated chain was packed diagonally across the "V groove" of the hexaene. This packing arrangement optimized contacts between hydrogens of the six double-bond carbons of the hexaenoic chain and methylene hydrogens of the saturated chain and led to a low cross-sectional area. In the second packing arrangement (Fig. 9, packing 6), the saturated chain was packed next to the external face of one plane of double bonds of the angle iron-shaped hexaene. MM2

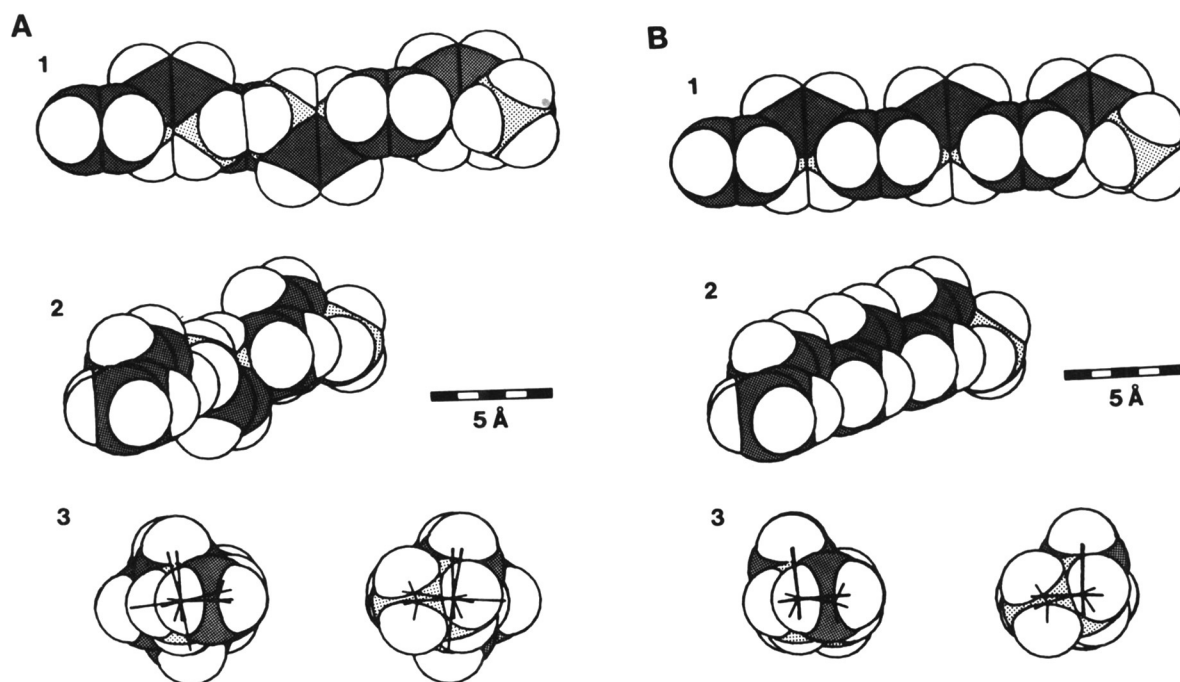


Fig. 6. Extended conformations of hexaenoic 19 carbon chains. Hexaenes generated as described in Fig. 4 are shown. A. A helical structure that results when all ten bond rotations about the five methylene carbons separating the double bonds are set to *skew* twists of the same sign (e.g., $+118^\circ$). B. An angle iron-shaped structure resulting from reversal of the signs of successive pairs of *skew* twists at the five methylene carbons separating the six double bonds (i.e., the sign sequence $++$, $--$, $++$, $--$, $++$). In both part A and part B, 1 is a longitudinal view in a plane defined by three of the six double bonds. The molecules are oriented left to right from carbon-1 to the ethyl terminus; 2 is an oblique view; 3 shows cross sections from opposite ends of the molecules. The left part of 3 is from the carbon-1 end, while the right part is from the ethyl terminus. Carbons and hydrogens are indicated as in Fig. 5.

rotated the molecules slightly about their long axes to relieve repulsion between methylene hydrogens on the two chains. Both types of packing arrangement showed a packing energy of about -13.3 kcal/mole, which is similar to that found for the optimum packing arrangements of two hexaenoic chains. Other lengthwise packings in which the saturated chain was packed diagonally across the external methylene hydrogens of the hexaene (Fig. 9, packing 7), or in which the narrow side of the saturated chain was packed diagonally across the groove of the hexaene (Fig. 9, packing 8), had higher energies because the hydrogen contacts were not quite so good.

We also studied a variety of mixed packings of three chains using models of identical short, angle iron-shaped polyenes and saturated hydrocarbons. One of these packings (Fig. 9, packing 9; Fig. 10B) combined the back-to-back, antiparallel arrangement of two hexaenes with the "V groove" packing arrangement of a hexaene and a saturated chain. The average packing energy per pair of interacting molecules lay in the same -12 to -13.5 kcal/mole range as was found for three polyunsaturated chains.

These studies of angle iron-shaped polyenes thus provided evidence that the angle-iron conformation is compatible with close packing arrangements involving both hexaenoic and saturated hydrocarbon chains. More importantly, they showed that optimal packing of two angle

iron-shaped hexaenes does not preclude optimal packing of these hexaenes with additional angle iron-shaped hexaenes and with saturated chains. Packings 4 and 9 in Fig. 9, in particular, raised the possibility that equal numbers of angle iron-shaped hexaenes and saturated molecules may tend to pack in a "stairstep" arrangement in which the hexaenes are aligned "back-to-back" and the "V groove" of each hexaene interacts with a saturated chain.

Interchain packing of helical hexaenes

We next sought to determine whether helical hexaenes pack equally well. The geometry of these hexaenes precludes "back-to-back" packing arrangements such as those formed by angle iron-shaped hexaenes. However, it seemed possible that helical hexaenes might form "edge-to-edge" packing arrangements, so we studied this type of packing in some detail. Furthermore, we examined the packing of helices that had first been minimized by MM2 and thus had torsion angles of 104° , and we also examined the packing of helices that had torsion angles of 118° . Several optimized packing arrangements involving such helices are shown in Fig. 11.

The most energetically stable packing arrangement for two identical helices was an interleaved arrangement of

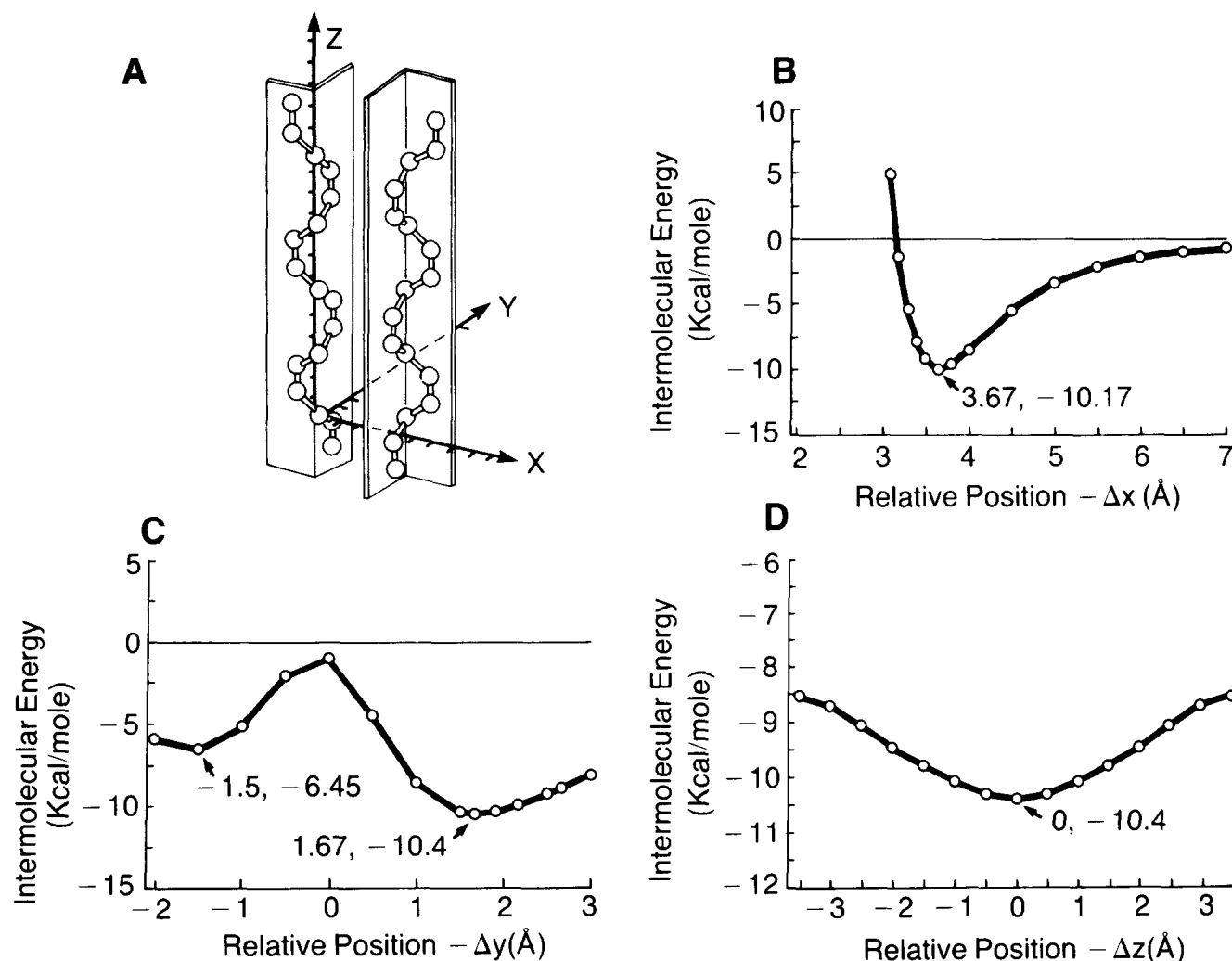


Fig. 7. Variation of the van der Waals intermolecular energy between two angle iron-shaped, 17 carbon hexaenes in the neighborhood of an optimum packing arrangement. The sequence of signs for the *skew* twists at the methylene carbons was $--, ++, --, ++, --$. Computer-generated models were moved relative to one another without altering the internal bond geometry. Successive searches along the x , y , and z axes were used to locate a local minimum energy packing, in this case a "back-to-back" arrangement of the angle iron conformations. A. Relative orientations of the molecules. Coordinate axes are defined relative to molecule 1 (left). The origin is located at the first methylene carbon (C-3); the z axis passes through all five methylene carbons. The plane corresponding to double bonds 2, 4, and 6 contains the negative x axis, while the positive y axis lies in the plane of double bonds 1, 3, and 5. The axis formed by the methylene carbons of molecule 2 (right) is parallel to the z axis. Molecule 2 has been rotated 180° about its own long axis. The planes formed by double bonds 1, 3, and 5 in each molecule are maintained parallel to one another. Direction vectors of all double bonds are approximately parallel to the z axis. B. Intermolecular van der Waals energy versus translation in x , for $y = 1.28 \text{ \AA}$, and $z = 0.00 \text{ \AA}$, respectively. The curve closely resembles the nonbonded potential for a single pair of atoms. C. Intermolecular van der Waals energy versus translation in y , for $x = 3.67 \text{ \AA}$, and $z = 0.00 \text{ \AA}$. The high point between local minima is caused by interaction of methylene hydrogens. D. Intermolecular van der Waals energy versus translation in z , for $x = 3.67 \text{ \AA}$, and $y = 1.67 \text{ \AA}$. The minimum occurs at $z = 0.00 \text{ \AA}$, the position where opposing sets of double bonds parallel to the y - z plane are in exact alignment.

helices that had torsion angles of 104° (Fig. 11, packing 1 and Fig. 12A). It had a packing energy (-13.07 kcal/mole) over 2 kcal/mole lower than that of a similar arrangement of two 118° torsion angle helices (-10.68 kcal/mole) and nearly as low as the -13.25 kcal/mole found for the comparable interleaved "edge-to-edge" packing of angle iron-shaped hexaenes. This low energy was a consequence of the geometry of 104° torsion angle helices. Only two double bonds (bonds 1 and 4) were missing from the lines of contact for these helices, whereas the comparable ar-

rangements of 118° helices (not shown) had three missing double bonds (bonds 1, 4, and 5). In addition, several methylene hydrogens in the 104° torsion angle helices substituted for the missing double-bond interactions.

Packings obtained for pairs of mirror-image helices showed non-interleaved "edge-to-edge" contacts and were less favorable than those obtained for identical helices. Even so, the packing energy of an arrangement of two 104° torsion angle helices (Fig. 11, packing 2) was once again lower than that of a comparable arrangement of two

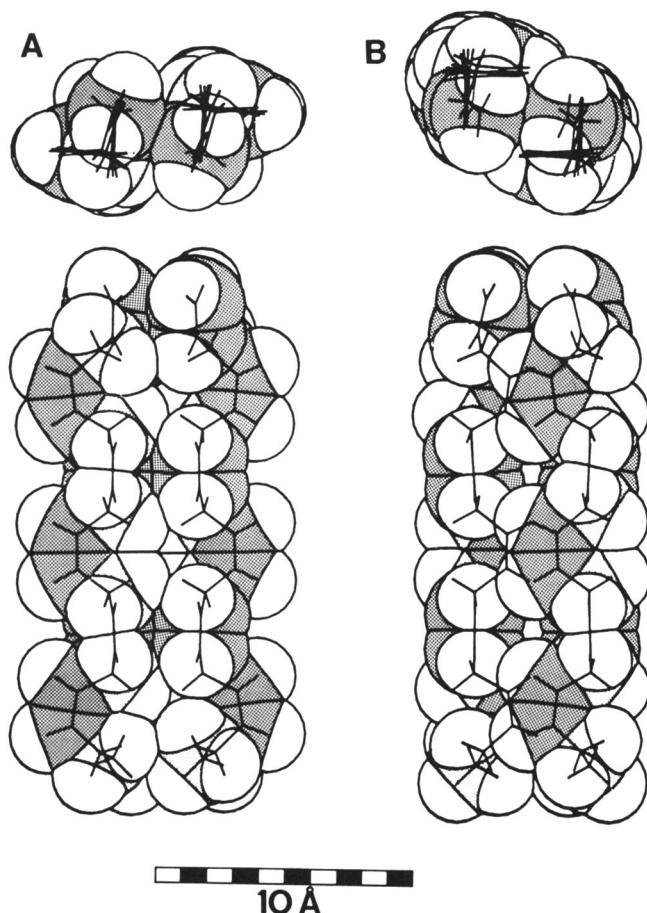


Fig. 8. Minimum energy packings of two angle iron-shaped, 19 carbon hexaenes. Space-filling views were generated using program SPMOL. Model hexaenes similar to that shown in Fig. 6B were used for the packings shown in both A and B. Cross sections are shown above; longitudinal sections are shown below. A. "Back-to-back" packing. B. "Edge-to-edge" packing. Note that vinyl hydrogens of bonds 1, 3, and 5 of one chain have close van der Waals contacts with vinyl hydrogens of bonds 2, 4 and 6 of the other chain, and vice versa. Carbons and hydrogens are indicated as in Fig. 5.

118° torsion angle helices (Fig. 11, packing 3).

Though two identical, 104° torsion angle helices could effectively use four pairs of their double bonds in an interleaved "edge-to-edge" packing, this left only two double bonds on the distal face of each helix available for packing with an additional helical chain. In contrast, a comparable packing arrangement of two 118° torsion angle helices used three pairs of double bonds and left three double bonds on each distal face available for packing with additional chains. Thus, 118° torsion angle helices were geometrically more suited for multiple chain packing arrangements than were 104° torsion angle helices. We therefore used 118° torsion angle helices in studies of "edge-to-edge" packings of three helices. To further optimize initial interchain contacts it was necessary to use a central helical chain that was a mirror image of the two neighboring chains. An interleaved arrangement of this type (Fig. 11,

packing 6 and Fig. 12C) had a packing energy of -10.27 kcal/mole, about 2 kcal/mole higher than that of three packed angle iron-shaped chains. Moreover, little distortion of the chains occurred, so the "edge-to-edge" contacts remained optimal. As anticipated, packing arrangements of three helices that had non-interleaved double-bond contacts (Fig. 11, packings 4 and 5) showed still higher packing energies. In addition, they showed chain distortion from the original 118° torsion angle conformation.

In studies of the packing of a helical hexaene with a saturated hydrocarbon, we again used helices that had 118° torsion angles. This allowed us to study packing arrangements that resembled the "V groove" packings of an angle iron-shaped hexaene and a saturated chain shown in Fig. 9, packings 5 and 8. Little distortion of either the helical chain or the saturated chain occurred in these packing arrangements (Fig. 11, packings 7 and 8), and the packing energies were 1.5 to 2 kcal/mole higher than for comparable packings of angle iron-shaped chains and saturated chains. The difference depended in part on fewer contacts of double bonds in the helix with the saturated chain. An arrangement similar to that shown in Fig. 11, packing 7, but involving a 104° torsion angle helix, yielded a minimum energy packing (not shown) with a packing energy nearly equal to that found for an angle iron-shaped chain and a saturated chain. However, during refinement, MM2 distorted the helix by shifting double-bond segments away from regions of contact with the saturated chain to create a "V groove."

Thus, a helical hexaene paired with a second helix or a saturated chain could achieve low energy packing arrangements comparable with those achieved by angle iron-shaped hexaenes. However, packings of three helices required steric compromises that led to packing energies that were considerably higher than those observed for angle iron-shaped polyenes. The same compromises would be expected to affect the packing of saturated chains with an array of helices, and only half as many double bonds would be available to interact with the saturated chains as for a comparable packing with angle iron-shaped polyenes. The results of these studies of angle iron-shaped hexaenes and helical hexaenes therefore suggest that in mixed arrays of saturated and polyenoic chains the potential of the angle iron-shaped conformation for promoting regular interchain packing arrangements of low packing energy may be considerably greater than that of the helical conformation.

Other interchain packing arrangements

To provide comparison data for the packing arrangements observed with angle iron-shaped and helical hexaenes, we modeled the packing of hairpin-shaped hexaenes and also that of saturated and/or monoenoic









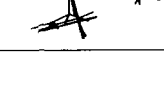
MOLECULE END VIEW	TOTAL ENERGY	PACKING ENERGY	AREA PER MOLECULE	MOLECULE END VIEW	TOTAL ENERGY	PACKING ENERGY	AREA PER MOLECULE
1 	18.87	-13.19	27.61	5 	12.94	-13.25	24.87
2 	19.17	-12.88	25.77	6 	12.93	-13.27	25.60
3 	20.10	-11.92	27.61	7 	14.08	-12.08	24.58
4 	13.65	-12.29	26.62	8 	13.88	-12.29	24.31
				9 	8.48	-13.20	24.39

Fig. 9. Packing energies and molecular areas for intermolecular arrangements involving identical angle iron-shaped, 19 carbon polyenes. Minimum energy packed arrays of two or three chains were obtained as described in Methods. These are shown as Dreiding model "wire-frame" cross sections. Total steric energies are given in kcal/mole. Calculation of packing energies (average kcal/mole interacting pair) and cross sectional areas (\AA^2) is described in Methods. Specific packings are as follows: 1. Back-to-back "antiparallel" packing of two polyenes as in Fig. 8A. 2. Edge-to-edge interleaved packing of two polyenes as in Fig. 8B. 3. Back-to-back "parallel" packing of two polyenes in which methylene hydrogens interact unfavorably. 4. Back-to-back "antiparallel" packing of three polyenes. 5. Saturated hydrocarbon packed optimally in the "V groove" of an angle iron-shaped polyene. 6. Saturated hydrocarbon packed on an external face of an angle iron-shaped polyene. 7, 8. Less favorable packings of a saturated hydrocarbon with an angle iron-shaped polyene. 9. Saturated hydrocarbon packed with two polyenes.

hydrocarbons. It seemed important to study the packing of hairpin-shaped hexaenes because, as mentioned previously, our studies of *isolated* hexaenes had shown that hairpin conformations had steric energies that were considerably lower than those of straight conformations (Fig. 4). We found, however, that hairpin-shaped hexaenes tend to pack poorly with other hairpin-shaped hexaenes or with saturated hydrocarbons. A pair of hexaenoic hydrocarbon chains in a hairpin conformation had to be packed with their flattest surfaces in apposition for best intermolecular contact (Fig. 13, packing 1). Even so, intermolecular interaction between the hairpin-shaped hydrocarbons was weak because there were few optimal hydrogen atom contacts. Many of the hydrogens were located on the irregular side of each molecule or in unfavorable orientations at the bends. The packing energy was therefore 3 to 4 kcal higher than for extended chains. Similarly, for an arrangement where an all-*trans* 16-carbon saturated chain was packed next to a 19-carbon, hairpin-shaped hexaene, there was only a small region of mutual contact, which led again to a high packing energy (Fig. 13, packing 2). These results suggested that hairpin-shaped conformations of DHA tend to preclude optimum interchain packing arrangements.

When we studied the packing of saturated hydrocarbons, we found, as anticipated, that saturated hydrocarbons packed very effectively. Fig. 10C and Fig. 13, packings 3–5 show packing arrangements refined by MM2 for two or three saturated chains that had been brought together in

a slightly offset arrangement to maximize contacts between the methylene hydrogens of the broad sides of the chains. Interestingly, the packing energies of these arrangements were quite similar to those found for hexaenoic, angle iron-shaped chains and for mixtures of these chains with saturated chains.

Studies of the packing of monoenoic hydrocarbons also led to an anticipated result. MM2 calculated that a monoenoic hydrocarbon that contained a *cis* double bond near the middle of the chain had a sharp bend at the double bond, in good agreement with the conclusions of others (e.g., 29–32). However, a conformation of slightly higher energy, the "jog form," was also possible. In this conformation, the two saturated portions of the chain were roughly parallel, though not colinear because of two bends in opposite senses adjacent to the two ends of the double bond. We studied this conformation because it seemed likely to favor interchain packing. Packing arrangements for two monoenes in the "jog form," refined by MM2, gave greatly distorted chain conformations. Though one of these arrangements, in which the double bond "jogs" were packed as closely as possible (Fig. 13, packing 6), yielded a packing energy only 1 kcal higher than the optimum values for hexaenes or saturated molecules, all other arrangements had packing energies at least 4 kcal higher. Packing arrangements for one monoenoic chain with one or two saturated chains are shown in Fig. 10D and Fig. 13, packings 7 and 8. Fig. 13 also shows that a single saturated chain helped to stabilize the conformation of the

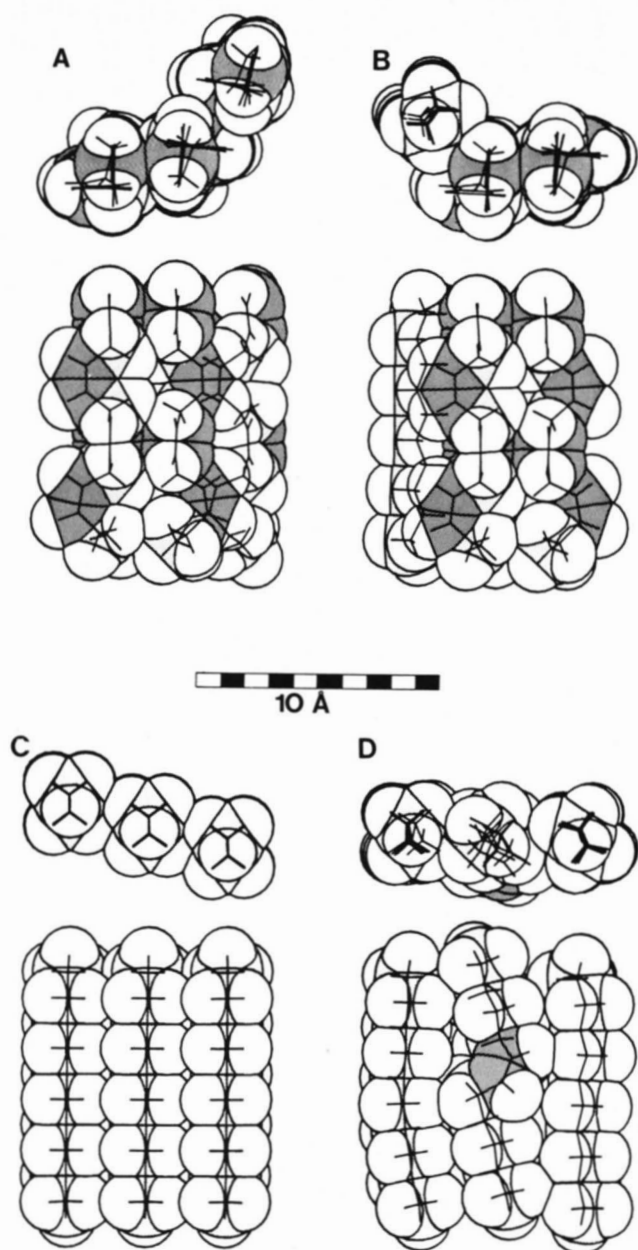


Fig. 10. Minimum energy packings for groups of three adjacent hydrocarbon chains of various types. Truncated chains were used throughout (see Methods). However, important structural features were preserved, such as the ethyl group at the chain terminus and the even number of double bonds in the polyunsaturated models of DHA. A. Three angle iron-shaped, 13 carbon tetraenes in an extension of the "back-to-back" packing shown in Fig. 8A. Note that this "stair-step" packing can be extended indefinitely to larger arrays of angle irons. B. A 10 carbon saturated hydrocarbon combined with two angle iron-shaped, 13 carbon tetraenes so that the latter pack "back-to-back" as in Fig. 8A while the saturated chain packs in the "V-groove" of one angle iron-shaped chain. C. Three 10 carbon saturated hydrocarbons packed so that the planes formed by their carbon atom chains are parallel, but offset so as to interlock the methylene hydrogens for maximum van der Waals interactions. D. An 11 carbon, monoenoic hydrocarbon (which mimics a longer oleoyl residue) packed between two 10 carbon saturated chains. Carbons and hydrogens are indicated as in Fig. 5.

monoene and yield a lower packing energy. However, the monoene could not achieve simultaneously optimum contacts when placed between two saturated chains, and the packing energy per interacting pair of molecules was consequently higher.

Because the results of these studies of saturated hydrocarbons and monoenoic hydrocarbons were generally consistent with published information (33), they supported the general validity of our modeling studies of the packing of hexaenes. Furthermore, the combined results of the packing studies of model saturated, monounsaturated, and polyunsaturated hydrocarbons suggested that the principal determinant of optimal chain packing may be geometrical regularity and compactness of a conformation rather than the presence or absence of *cis* double bonds per se.

Interchain packing in diacylglycerols

Having investigated the packing of separate hexaenoic hydrocarbon chains, we sought to determine whether the packing arrangements found for these chains might be possible also for the covalently linked acyl chains of phospholipids. However, limitations of the MM2 modeling programs available to us precluded the study of entire phospholipids (see Methods), so we examined the interaction of acyl chains in diacylglycerols instead. Furthermore, because we were primarily interested in the DHA of nerve membranes, which is mainly found in PE, we used as a model the conformation of the diacylglycerol moiety reported for crystals of dilauroyl PE (34). In this conformation the *sn*-1 acyl chain and the glycerol moiety are aligned along a single axis. The *sn*-2 acyl chain initially projects outward from this axis at an angle of about 90°, then bends to become parallel to the *sn*-1 chain.

To determine whether a diacylglycerol containing a saturated acyl chain in the *sn*-1 position and an angle iron-shaped DHA chain in the *sn*-2 position could assume a similar conformation, we used the method developed by Go and Scheraga (35) and the program FINDTORSIONS (see Appendix II) to identify sequences of torsion angles that would accommodate parallel chain packings. Then we applied the steric and chemical criteria defined in Appendix II to select molecular conformations that could be refined further using MM2. We found that several solutions of the Go and Scheraga (35) equations were possible for various relative orientations of the acyl chains (Fig. 14). Some orientations, however, produced no solutions, and only one solution (Fig. 15C, Table 3) was compatible with the structure of crystalline dilauroyl PE. This solution yielded torsion angles for the region of the 90° bend that were in close agreement with those reported for dilauroyl PE, except for β_3 which was altered to compensate for the geometry of the double bond at β_6 . Sig-






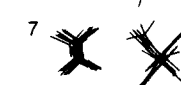

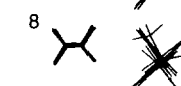
MOLECULE END VIEW	TOTAL ENERGY	PACKING ENERGY	AREA PER MOLECULE	MOLECULE END VIEW	TOTAL ENERGY	PACKING ENERGY	AREA PER MOLECULE
1 	17.93	-13.07	30.11	5 	17.15	-9.17	30.04
2 	21.88	-8.96	31.16	6 	15.71	-10.27	32.57
3 	25.80	-4.88	32.90	7 	13.86	-11.69	27.03
4 	19.86	-7.10	32.57	8 	15.12	-10.38	26.39

Fig. 11. Energies and molecular areas for packed arrangements involving helical polyenes. Helical conformations of polyunsaturated hydrocarbon chains as in Fig. 6B were combined with one another or with all-*trans* saturated chains in packed arrays that were optimized using MM2. Dreiding model outlines for these optimum packings are shown. Total steric energies are given in kcal/mole. Packing energies were calculated as described in Methods and are given as average kcal/mole per interacting pair of molecules. Cross-sectional areas are in average Å²/molecular component. To describe the somewhat complex packing of helices, we use the following notation: L, C, and R designate left, center, and right molecules in the Dreiding outlines. Top and bottom edges refer to the two lines of contact of double bonds, perpendicular to the page, between adjacent helices. Opposed contacts occur between double bonds at the same level perpendicular to the page, while interleaved contacts occur between double bonds at neighboring levels (see Fig. 12A for example of interleaved contacts). A 104° helix is the MM2 minimized form with a screw repeat every 3.3 double bonds, while a 118° helix has been twisted back to the form that repeats every 4 double bonds. The following packings are shown: 1. 104° helices. R identical to L but rotated 180°. Interleaved contacts: top edge 3L-2R, 6L-5R; bottom edge 2L-3R, 5L-6R. 2. 104° helices. R mirror image of L. Opposed contacts: top edge 2L-2R, 5L-5R; bottom edge 3L-3R, 6L-6R. 3. 118° helices. R mirror image of L. Opposed contacts: top edge 2L-2R only; bottom edge 3L-3R, 6L-6R. 4. 118° helices. C mirror image of L and R. Opposed contacts: top edge 3L-3C, 4C-4R; bottom edge 2L-2C; 1C-1R. 5. 118° helices. C mirror image of L and R. Opposed contacts: top edge 4L-4C, 1C-1R; bottom edge 3L-3C, 2C-2R. 6. 118° helices. C mirror image of L and R. Interleaved contacts: top edge 3L-2C, 2C-3R; bottom edge 2L-3C, 3C-2R. 7. Broad face of all-*trans* saturated chain oriented toward 118° helix. Contacts of saturated chain hydrogens with double bonds: top edge, bonds 1, 5; bottom edge, bonds 2, 6. 8. Narrow face of all-*trans* saturated chain oriented toward 118° helix. Contacts of saturated chain hydrogens with double bond: top edge, bonds 1, 5; bottom edge, bonds 2, 6.

nificantly, the solution corresponded to a chain packing arrangement that was strikingly similar to that shown in Fig. 9, packings 5 and 9, and in Fig. 10B for individual saturated and angle iron-shaped chains. This solution is also compatible with a diacylglycerol molecule containing a helical model of DHA in the *sn*-2 position (not shown).

The diacylglycerol containing a saturated acyl chain in the *sn*-1 position and an angle iron-shaped DHA moiety in the *sn*-2 position had a conformation that was almost as regular as that found for crystalline dilauroyl PE (compare Figs. 15A and C and see Table 4). The tight bend in the *sn*-2 chain caused essentially no distortion in the overall shape of the diacylglycerol molecule. The methylene-interrupted double-bond structure was straight, as observed previously for packed individual chains, while the ethyl group at the DHA chain terminus caused relatively little deformation. The highly regular conformation of the DHA-containing diacylglycerol seemed likely to favor the formation of regular, tightly packed intermolecular arrays.

To determine whether a diacylglycerol containing another polyenoic fatty acid might show an equally regular conformation, we studied a diacylglycerol that contained a saturated acyl chain in the *sn*-1 position and an angle iron-shaped arachidonic acid moiety in the *sn*-2 position. We again applied the Go and Scheraga proce-

dure (35) to identify possible torsion angles proximal to the double-bond sequence, but fixed the θ_1 and β_7 bonds and obtained solutions for β_1 through β_6 . We could thus require parallelism of the acyl chains as well as an orientation of the glyceryl-free hydroxyl group that was compatible with the conformation of crystalline dilauroyl PE.

We obtained twelve sets of solutions. All achieved parallelism of the acyl chains by forming large loops in the β_1 - β_6 region, and most showed at least one unfavorable torsion angle in a nearly eclipsed conformation. We next used MM2 to refine the two solutions of lowest initial energy and the two of highest initial energy. All four refinements led to minimum energy conformations 4 to 6 kcal higher than that obtained for a diacylglycerol containing an angle iron-shaped model of DHA of comparable chain length. The minimized conformations of arachidonic acid-containing diacylglycerol had a similar shape and still contained broad loops at the bend in the *sn*-2 chain. Table 3 contains conformational details, while Fig. 15B shows two views of the lowest-energy conformation. This conformation was considerably less regular than that of the diacylglycerol containing an angle iron-shaped DHA moiety in the *sn*-2 position (Fig. 15C, Table 4). Part of the irregularity was due to the Δ_5 double bond in the arachidonic acid moiety. Whereas the Δ_4 double

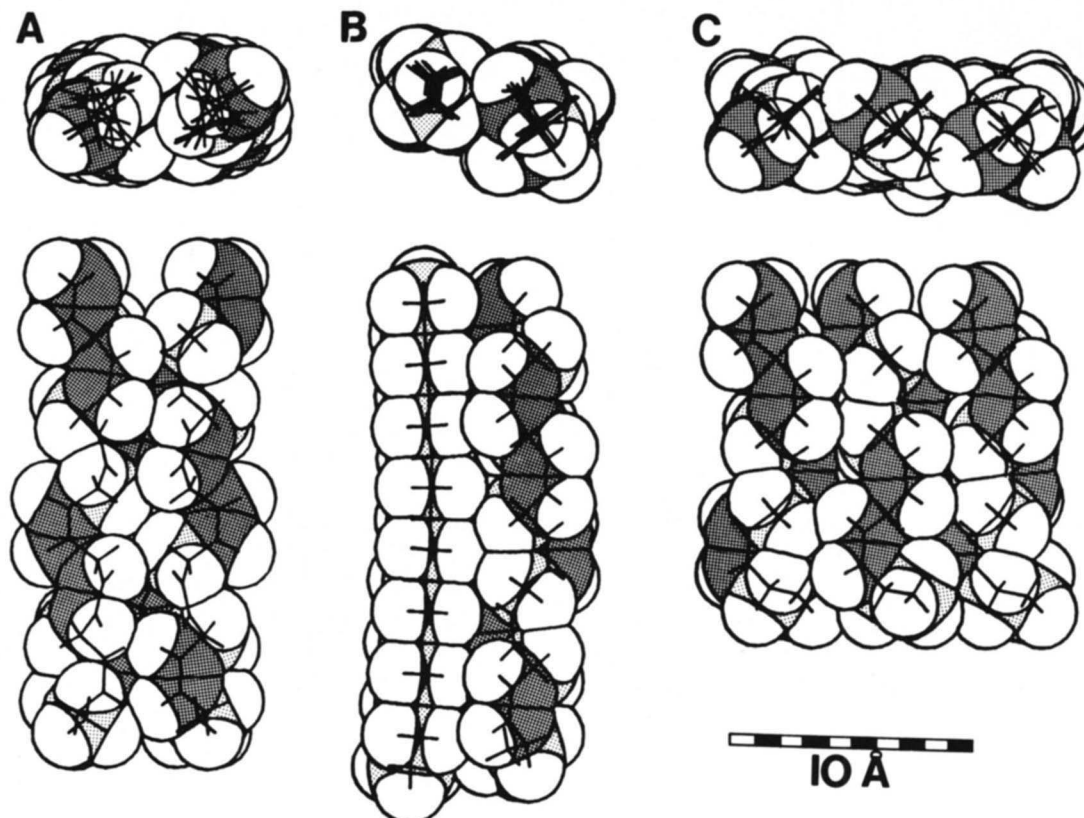


Fig. 12. Minimum energy packings involving polyunsaturated hydrocarbons in the helical conformation. A. Two 19 carbon, hexaenoic helices with the second chain rotated 180° about its long axis relative to the first chain. B. A 16 carbon saturated chain and a helical, 19 carbon hexaene. The resistance of the saturated chain to deformation provides a template which helps maintain the helix in its original regular form. However, this prevents distortions of the helix that could compensate for the lack of interaction between the saturated chain and double bonds 3 and 4. C. Three 13 carbon tetraenoic helices, side by side. The central chain is rotated 90° about its axis relative to the outer chains. This permits maximum "edge-to-edge" van der Waals contact of three double bonds of this chain with each of the other chains. Carbons and hydrogens are indicated as in Fig. 5.

bond in DHA was compatible with a smooth, sharp 90° bend in the chain, the presence of an additional methylene group proximal to the $\Delta 5$ double bond precluded such a bend in arachidonic acid. Another factor contributing to the irregularity was the 5-carbon saturated terminal segment of the arachidonic acid chain. In contrast with the terminal ethyl group of DHA, it appeared to be large enough to interfere significantly with interchain packing.

The results of this comparative study of diacylglycerols containing two different polyunsaturated fatty acids emphasized the potential conformational importance of two structural features that occur *together* only in DHA. Thus, DHA alone contains a polyenoic sequence that is *a*) initiated by a $\Delta 4$ double bond, and *b*) terminated by an *n*-3 double bond. Both features seem to be required for optimum regularity of a diacylglycerol containing an *sn*-2 polyunsaturated fatty acid.

DISCUSSION

Computer modeling studies of phospholipids have generally focused on the conformation and packing prop-

erties of saturated PCs. Only a few studies of mono-unsaturated phospholipids and/or PE head groups have been reported (36–38), and polyunsaturated phospholipids have so far received almost no attention (see, however, refs. 8, 28). One strategy has been to use quantum calculations or empirical force fields to determine the lowest steric energy of an isolated molecule or molecular fragment and thereby identify its probable optimum conformation (37, 39, 40). A complementary strategy has been to use simplified structural models and force fields to examine the packing geometry and intermolecular interactions of arrays of molecules in monolayers and bilayers (36, 41–43). Several investigators have combined these strategies, first determining conformations of single molecules, then using them as components of packing systems of various degrees of complexity (44–46).

The force fields used have invariably been restricted. Early work often limited the force field to a simple Lennard-Jones van der Waals potential (39). Later work included torsional; electrostatic, and hydrogen bonding potentials and, in one set of studies (46), also lone pair electrons on phosphate oxygens. But a rigid molecular framework of fixed bond lengths and angles has always been assumed.

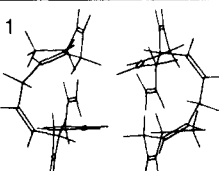
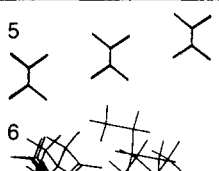
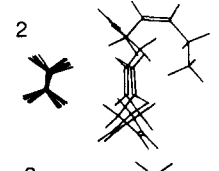

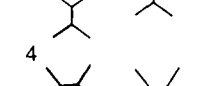

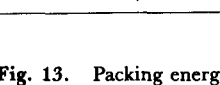
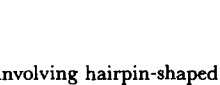
MOLECULE END VIEW	TOTAL ENERGY	PACKING ENERGY	AREA PER MOLECULE	MOLECULE END VIEW	TOTAL ENERGY	PACKING ENERGY	AREA PER MOLECULE
1 	13.65	-9.95	57.83	5 	1.82	-12.22	20.29
2 	12.02	-9.57	41.69	6 	7.51	-11.71	33.94
3 	6.42	-12.88	22.17	7 	8.98	-12.37	25.58
4 	6.72	-12.59	20.22	8 	5.89	-11.06	23.01

Fig. 13. Packing energies and molecular areas for packing arrangements involving hairpin-shaped hexaenes, saturated hydrocarbons, and mono-unsaturated hydrocarbons. Minimum energy conformations for hairpin conformations of polyunsaturated chains, all-*trans* saturated hydrocarbon chains, or monounsaturated chains in the jog form were combined in various packed arrays, then reoptimized using MM2. Dreiding model outlines of the final packed arrays are shown. Total steric energies are given in kcal/mole, packing energies in average kcal/mole per interacting pair, and cross-sectional areas in Å² (as described in Methods). The following packings are listed: 1. Two hairpin-shaped polyenes as in Fig. 5 were packed after rotating the molecule on the right by 180°. Double bonds 1, 2, 3, and 6 of each molecule were initially aligned perpendicular to the plane of the page, while double bonds 4 and 5 formed the hairpin loops. Double bonds 2 and 3 of each molecule are packed close to double bond 6 of the opposite molecule. 2. A hairpin-shaped polyene packed with a saturated chain. Double bonds 1, 3, 4, and 5 form the sides of a rectangle lying in a vertical plane perpendicular to the page, and create a fairly flat surface against which the saturated chain can pack. 3-5. Packings of saturated chains. 6. Packing of two monoenes that initially had identical orientations. Note that MM2 greatly distorted the molecule on the right. 7. Packing of a monoene with a saturated chain. 8. Packing of a monoene with two saturated chains.

The present study thus differed from earlier studies, not only because we focused on DHA and sought to identify conformations of this fatty acid that might influence the packing of PE and PS in nerve membranes, but also because we used MM2. The use of this program allowed a full molecular mechanics force field to be applied to lipid modeling for the first time. A particularly valuable feature of MM2 allows simultaneous adjustment of bond lengths and angles along with other force field parameters. This tends to improve geometric packing because relaxation of bond geometries can lead to a large decrease in the energy of repulsion for 1,4 (short range) van der Waals interactions.

The results obtained in our study support the possibility that the methylene-interrupted double-bond structure of DHA can be an important determinant of phospholipid packing in membranes. They show that this structure is compatible with two essentially straight conformations. In one the double-bond carbons project outward from a straight chain axis in a helical arrangement (Fig. 6A); in the other they project outward to form an angle iron-shaped structure (Fig. 6B).

The angle iron-shaped conformation may have a special potential for interchain packing because its two planar surfaces can pack "back-to-back" with the planar surfaces

of other angle iron-shaped molecules, while its interplanar "V groove" can align with a saturated chain. Such packing arrangements involve considerably more interchain contact than can occur among packed helices or between a helical chain and a saturated chain. They are therefore associated with low interchain packing energies.

It is important to note that the angle iron-shaped conformation of DHA is compatible with a diacylglycerol conformation that has nearly the same cross-sectional area and is almost as regular as the conformation reported for the diacylglycerol moiety of crystalline dilauroyl PE (34). Regularity is possible when the saturated acyl chain is in the *sn*-1 position and the DHA chain is in the *sn*-2 position because the $\Delta 4$ double bond in DHA allows a tight bend to occur in the initial part of the chain and because the ethyl group at the chain terminus causes only minimal distortion of the chain axis. The *sn*-1 and *sn*-2 acyl chains form an intramolecular packing arrangement that is essentially identical to the intermolecular chain packing found to be optimal for an angle iron-shaped hexaene and a saturated hydrocarbon (compare Figs. 10B and 15C). Because the saturated chain packs along the "V groove" of the angle iron-shaped chain, the two planar faces of the polyunsaturated chain remain free to participate in intermolecular interactions. "Back-to-back" intermolecular

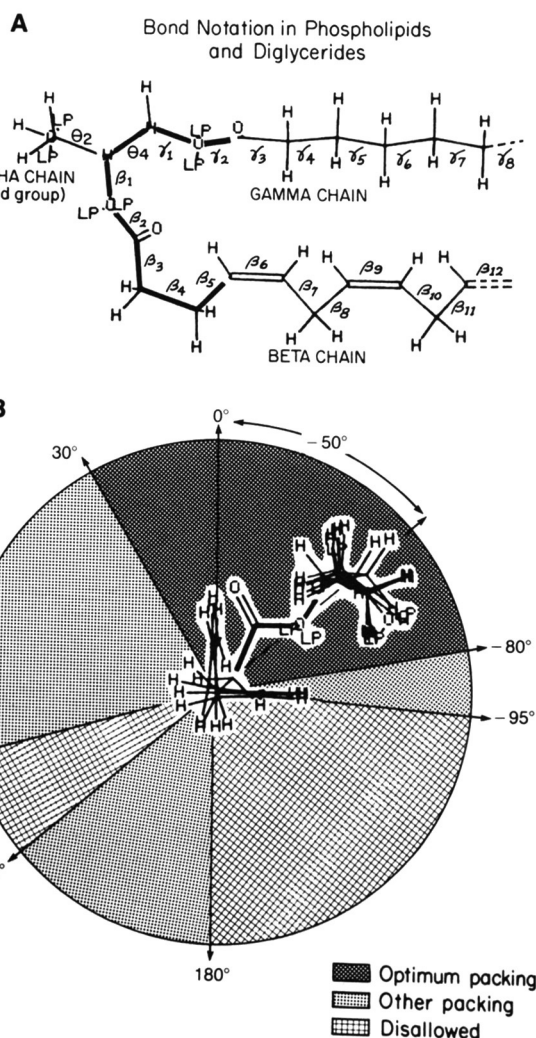


Fig. 14. Structure, bond notation, and acyl chain conformation in a mixed chain diacylglycerol containing a model of an *sn*-2 DHA chain. **A.** The standard phospholipid bond notation of Sundaralingam (17), as adapted to a diacylglycerol containing an *sn*-1 saturated chain and an *sn*-2 DHA chain. The heavy lines corresponding to portions of the β and γ chains and the glyceryl moiety denote bonds that define a bridging section between the two acyl chains. The torsion angles of these bonds must be adjusted to allow parallel packing of the two chains. Allowed sets of angles may be calculated by the method of Go and Scheraga, as described in Appendix II. **B.** Orientations of paraxial acyl chains in the same mixed chain diacylglycerol. Ranges of position angles yielding bridge bond torsion angles similar to those found by Elder et al. (34) for dilauroyl PE are indicated by dark shading. Lighter shading indicates ranges where unrelated torsion angle solution sets exist. Although such solutions are possible geometrically, they do not produce conformations that are reasonable sterically or chemically (see Appendix II). Cross-hatching indicates regions where torsion angle solution sets do not exist. The 0° position is defined as lying along the face of the central angle iron-shaped DHA residue that contains the terminal ethyl group. Positive angles are measured in a counterclockwise direction as viewed from the acyl ester end of the chains. The plane of the carbon atoms in the saturated chain is normal to the line joining the two chain axes for all position angles. The superimposed molecular outline shows the actual MM2 minimum energy structure for a diacylglycerol molecule containing decanoic acid in the *sn*-1 position and a 16 carbon, tetraenoic model of DHA in the *sn*-2 position. (This model contained a $\Delta 4$ double bond as well as a terminal ethyl group).

interactions such as those shown in Figs. 8A and 10A are compatible with a highly ordered packing array, which might be favored in compressed monolayers (**Fig. 16A**). Diacylglycerols containing helical DHA might form an ordered array that would be limited to less favorable packings involving partial edge-to-edge contacts between helices (**Fig. 16B**).

An ordered packing array of PE molecules, such as that shown in **Fig. 16A**, would be expected to influence the packing of lipids on the opposite side of a membrane bilayer. It is of interest therefore that nearly four-fifths of the DHA of brain diacyl PE is associated with stearic acid (47). If the conformations of 1-stearoyl-2-docosahexaenoyl PE and 1-palmitoyl-2-docosahexaenoyl PE in brain membranes are similar to that of the model diacylglycerol shown in **Fig. 15C**, then the lengths of the saturated chains would exceed those of the associated DHA chains by about 4.5 Å and 1.9 Å, respectively. The non-polar face formed by the ends of the packed chains would accordingly be uneven and perhaps provide a possibility for interdigitation with the chain ends of opposing lipids such as gangliosides.

The conclusions of the present study are limited. They apply only to DHA-containing phospholipids that show a diacylglycerol conformation similar to that reported for crystalline dilauroyl PE. The DHA must be in the *sn*-2 position, and a saturated fatty acid must be in the *sn*-1 position. In addition, the phospholipid head group should probably be ethanolamine or serine. Choline is likely to be too large to be compatible with this type of conformation, as suggested by the very different crystal structures that have been reported for disaturated PE and PC (18). Other factors that would be expected to influence the type of interchain packing arrangements predicted in the present study include: *a*) the relative content of DHA-containing PE in a phospholipid mixture or packed monolayer, *b*) temperature, and *c*) the content of proteins and lipids in the two sides of a membrane bilayer.

These limitations should be kept in mind while evaluating published data on lipid and membrane structure that might support or refute the predictions of our modeling studies. The data that are currently available, reviewed recently by Stubbs and Smith (8) and by Dratz and Deese (3), unfortunately relate primarily to PCs. Thus, it is difficult to find specific and unequivocal information concerning DHA in the PE and PS species that account for much of this fatty acid in biological membranes.

To our knowledge the only experimental study of DHA-containing PE that has been published so far is that of Dekker et al. (48). These investigators studied hexagonal H_{II} phase transitions for a number of phospholipids including didocosahexaenoyl PE. They found that this type of PE is in the hexagonal H_{II} phase for all temperatures

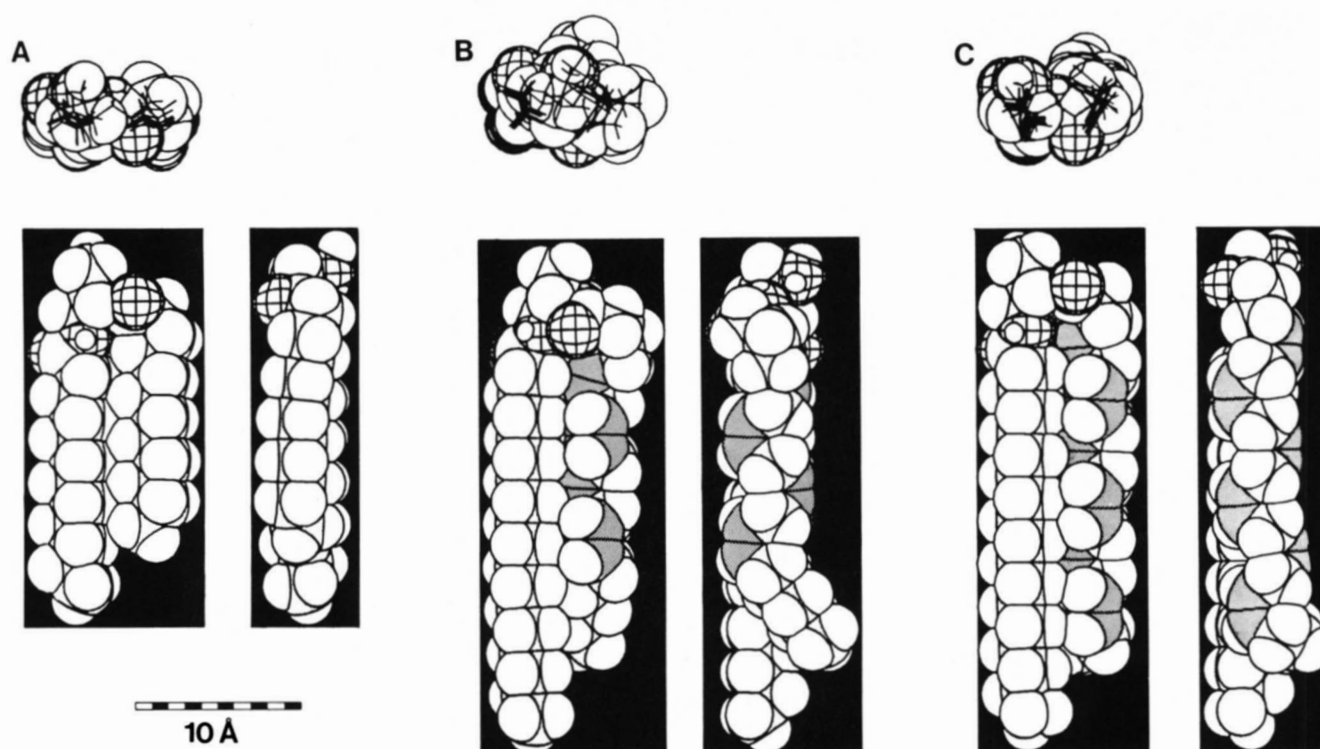


Fig. 15. Comparison of minimum energy diacylglycerol conformations. A. Dilauroylglycerol derived from the X-ray structure for dilauroyl PE determined by Elder and coworkers (34). The PROPHET interface to the Cambridge Crystal File (56) was used to access the atomic coordinates for the unit cell and convert them directly to the molecular model. The phosphorylethanolamine head group was replaced by a hydroxyl group to yield the diacylglycerol, then MM2 was used to refine the model. There were only minor differences between the MM2 model and the original experimental conformation. B. The lowest energy conformation of several models of 1-stearoyl-2-arachidonoyl glycerol initially determined by program FINDTORSIONS and then refined using MM2. Acyl chains were initially constrained to pack in the optimum way found for angle iron-shaped chains and saturated chains (Fig. 9, packing 5). C. The conformation of 1-stearoyl-2-docosahexaenoyl glycerol that corresponded most closely to the dilauroyl PE structure. Again, FINDTORSIONS was used to determine this structure under the same constraints as in part B for acyl chain packing, and MM2 was used to refine it. Carbons and hydrogens are indicated as in Fig. 5. Oxygens are indicated by cross hatching, lone pair electrons by small unshaded circles.

above -30°C , which is consistent with the classical idea that greater unsaturation implies greater membrane fluidity. Though didocosaehaenoyl PE falls outside of the limited area covered by our modeling studies, the initial saturated segment of the *sn*-1 DHA chain would be expected to produce a kink or a jog where it joins the chain's polyunsaturated segment. Even if the polyunsaturated segment of the *sn*-1 chain were to have an angle iron-shaped or helical conformation, the lack of colinearity with the saturated segment would be expected to be associated with an increased effective cross-sectional area of the PE molecule, either in the polyunsaturated region or in the saturated and ester segments linking the two acyl chains.

Though published studies of DHA-containing PC also fall outside the area covered by our modeling studies, they may provide useful hints regarding the general effects of an *sn*-2 DHA chain in phospholipids. Early results from monolayer studies by Ghosh, Williams, and Tinoco (49)

and by Demel, Geurts Van Kessel, and VanDeenen (50) showed that introduction of one double bond in the *sn*-2 chain of PC greatly increases the molecular area, but that subsequent double bonds cause only minor additional increments. In fact, for 1-stearoyl-2-docosahexaenoyl PC there is a small condensing effect relative to 1-stearoyl-2-oleoyl PC. These findings imply that the packing of DHA chains at the *sn*-2 position in PC is no more random than that for monounsaturated chains, and may actually show a fair amount of order.

Information on phase transition temperatures supports this view. The melting temperature of 1-palmitoyl-2-palmitoleoyl PC was determined to be -10°C while the average for 1-palmitoyl-2-docosahexaenoyl PC was -6°C (51); and recent data for a series of PCs containing stearic acid in the *sn*-1 position and oleic acid through arachidonic acid in the *sn*-2 position show a minimum melting temperature of -16°C for linoleic acid, and then a leveling off to about -12°C for more unsaturated species (52). More-

TABLE 3. Comparative torsion angles for model 1-saturated-2-polyunsaturated diacylglycerols and a 1,2-disaturated diacylglycerol derived from X-ray structure for dilauroyl PE

Bond	Diacylglycerol Species			Bond	Diacylglycerol Species		
	1,2-Dilauroyl	1-Stearoyl-2-docosa-hexaenoyl	1-Stearoyl-2-arachidonoyl		1,2-Dilauroyl	1-Stearoyl-2-docosa-hexaenoyl	1-Stearoyl-2-arachidonoyl
α_1'	-154.4	-179.4	-178.7	β_{19}		117.0	178.2
θ_1	-52.1	-57.0	-59.2	β_{20}		123.0	-179.2
θ_2	65.4	63.2	61.5	β_{21}		-0.2	-178.4
θ_3	-172.3	-170.2	-171.2	β_{22}		-93.6	
θ_4	69.1	68.7	69.4	β_{23}		178.5	
β_1'	-141.5	-139.1	-92.3	γ_1	-178.3	-161.2	-177.8
β_1	96.6	98.1	146.9	γ_2	172.7	-178.0	175.9
β_2	179.3	179.2	-168.6	γ_3	178.9	-177.4	-159.1
β_3	-118.5	-90.3	-61.6	γ_4	-171.4	-176.0	173.4
β_4	64.8	68.9	-77.9	γ_5	-172.6	-179.7	-176.5
β_5	-178.1	-171.5	74.6	γ_6	174.0	-177.9	-179.6
β_6	-174.8	-0.1	-176.7	γ_7	-178.7	-178.9	179.1
β_7	175.9	121.1	0.8	γ_8	-177.0	179.9	-179.6
β_8	-173.4	110.4	123.1	γ_9	-177.9	179.8	-179.2
β_9	178.2	0.1	142.9	γ_{10}	-177.8	179.3	-178.6
β_{10}	-179.4	-124.9	-0.1	γ_{11}	172.6	179.9	-178.6
β_{11}	-177.5	-120.8	-115.3	γ_{12}	160.9	179.0	179.3
β_{12}	-179.5	0.1	-123.4	γ_{13}	-180.0	-179.5	-177.3
β_{13}	-180.0	125.3	0.0	γ_{14}		-179.4	176.8
β_{14}		118.1	117.3	γ_{15}		179.0	179.8
β_{15}		0.0	129.1	γ_{16}		176.5	179.7
β_{16}		-124.9	-0.2	γ_{17}		-177.8	179.9
β_{17}		-124.3	-121.4	γ_{18}		179.9	-179.7
β_{18}		-0.2	-178.4	γ_{19}		-180.0	-178.4

Principal torsion angles are listed for the carbon and ester backbones of the diacylglycerols, employing the notation of Sundaralingam (17). The models are minimum energy conformations calculated using MM2. The conformation about the glyceryl carbons is essentially similar for all diacylglycerols (θ_1 - θ_4). The dilauroylglycerol and 1-stearoyl-2-docosahexaenoylglycerol are also very similar in the region of the β chain bend (β_1 - β_5), except for β_3 . The γ chains of the two diacylglycerols are both close to an all *trans* conformation, with the exception of γ_1 in the 1-stearoyl-2-docosahexaenoylglycerol model. Rotation of that bond by about -20°C promotes better packing of the β and γ chains. The polyunsaturated part of the DHA model has torsion angles about the methylene carbons that are all within $\pm 8^\circ$ of the $\pm 118^\circ$ optimum. In contrast, the 1-stearoyl-2-arachidonoyl model differs considerably for all bonds in the β chain bend (β_1 - β_5) to an extent that may increase significantly the torsional part of the steric energy. In addition, there are two large deviations in the polyunsaturated chain (β_9 - β_{15}) from the optimum 118° torsion angle.

over, Deese et al. (51) found that plots of order parameter versus temperature for unsaturated PC molecules containing an *sn*-1 palmitoyl residue, labeled with a terminal CD_3 group, showed that the 1-palmitoyl-2-palmitoleoyl species had a broad melting range with no hysteresis. In contrast, the 1-palmitoyl-2-docosahexaenoyl species was characterized by a narrow gel-to-liquid-crystal transition, with hysteresis between the cooling and heating curves. This evidence of cooperativity is consistent with chain order.

When Paddy et al. (53) employed a deconvolution method to determine the order parameters and relaxation times for all segments of a perdeuterated *sn*-1 palmitoyl chain in dipalmitoyl PC, 1-palmitoyl-2-palmitoleoyl PC, and 1-palmitoyl-2-docosahexaenoyl PC, they found that the *sn*-1 chain as a whole was more resistant to deformation when paired with a DHA chain than when paired

with a palmitoleoyl chain. This result is consistent with the possibility that a rigid double-bond geometry in DHA limits the motion of individual segments in the neighboring chain.

Finally, Dratz and Deese (3) have outlined results, yet to be published in detail, of NMR studies of 1-palmitoyl-2-docosahexaenoyl PC, perdeuterated at the double bonds of the DHA chain. The NMR spectrum appears to consist of a narrow line showing no splitting. This can occur if the C-D bonds show an ordered orientation at the so-called "magic angle" of 54° to the bilayer normal (54). Dratz interprets these data as being consistent with a DHA helical conformation oriented perpendicular to the bilayer. However, the data are also consistent with an angle iron-shaped conformation of DHA. Our calculations using the geometry of MM2-minimized models of both conformations yield an angle of about 52°C between the

TABLE 4. Molecular areas for lateral cross sections through various diacylglycerols and phospholipids

Molecule/Section Location	Bonds Included in Section	Mean Area (Å ²)	
		Per Section	Per Acyl Chain
Dilauroyl PE			
Whole molecule projection	all bonds	74.32	N/A
Glyceryl diester and β chain bend	γ ₂ -γ ₁ , θ ₄ , θ ₂ , β ₁ -β ₄	53.62	26.81
Head group	α ₁ -α ₆	39.90	N/A
Acyl chains	γ ₃ -γ ₁₄ , β ₅ -β ₁₄	46.74	23.37
1,2-Dilauroylglycerol			
Proximal	γ ₅ -γ ₁ , θ ₄ , β ₁ -β ₉	49.22	24.61
Distal	γ ₇ -γ ₁₃ , β ₁₂ -β ₁₃	42.32	21.16
1-Stearoyl,2-docosahexaenoylglycerol			
Proximal	γ ₅ -γ ₁ , θ ₄ , β ₁ -β ₉	49.54	24.77
Middle	γ ₇ -γ ₁₁ , β ₁₂ -β ₁₅	46.29	23.15
Distal	γ ₁₂ -γ ₁₉ , β ₁₈ -β ₂₃	43.67	21.83
1-Stearoyl,2-arachidonoylglycerol			
Proximal	γ ₆ -γ ₁ , θ ₄ , β ₁ -β ₆	54.57	27.28
Middle	γ ₇ -γ ₁₂ , β ₁₃ -β ₁₆	46.07	23.04
Distal	γ ₁₃ -γ ₁₉ , β ₁₇ -β ₂₁	51.28	25.64


Molecular models, having conformations optimized by the MM2 program, were oriented so that the axes of the acyl chains were parallel to the z-axis. Program MOLSECTION was used to determine the area for the projection of each cross section on the x-y plane. The approximate thickness of each cross section is indicated approximately by the included bonds. MM2 van der Waals radii were used. The large, 'soft' hydrogens used in this parameterization cause the areas to be from 5–10 \AA^2 larger than those determined experimentally for condensed monolayers, bilayers, or crystal structures. However, the relative areas are of interest. Both the disaturated and the DHA-containing diacylglycerols have relatively constant areas over the entire lengths of the molecules. (The somewhat larger values for the proximal portions, i.e., those portions that are closest to the glycerol moiety, are caused by the ester oxygen atoms.) In contrast, the proximal and distal sections of the molecule containing arachidonic acid are significantly larger because of an enlarged loop at the 90°C bend in the β chain and a tilted ω_6 saturated tail. The values for dilauroyl PE were calculated using MM2 van der Waals parameters for the structure of Elder et al. (34) obtained from the Cambridge Crystal File. The somewhat larger glyceryl diester cross section includes the C₁ methylene group and slightly different torsion angles in the $\beta_1-\beta_6$ region. The head group is seen to be slightly smaller in cross section than the acyl chains. The large total projected area for dilauroyl PE is caused by the lateral offset of the head group from the acyl chains. N/A, not applicable.

vinyl C-H bonds and the axis formed by the methylene carbons (not shown).

Thus, our models seem consistent with the limited experimental data that are available on the conformations and packing properties of polyunsaturated lipids. However, further work will clearly be needed to extend the models, test their validity, and explore their implications. For example, it will be important to conduct further modeling studies using programs that accommodate intact molecules of 1-stearoyl-2-docosahexanoyl PE and PS. A major question that needs to be addressed is whether the regular acyl chain packing arrangements observed in the present study are consistent with, or may even be favored by, headgroup interactions among PE molecules or divalent cation salts of PS.

It will be important also to conduct specific experimental studies of 1-stearoyl-2-docosahexanoyl PE and PS. A deuterium NMR study in which the *sn*-2 chain is either labeled selectively or perdeuterated would be of obvious interest. It also might be possible to obtain im-

portant information using Fourier transform IR. In addition, a determination of the molecular areas of PE and PS in a monolayer might be used to test our prediction that extended molecules of PE and PS, characterized by acyl chains that are perpendicular to the monolayer surface, form tightly packed arrays.

Experimental verification of this possibility would raise a number of questions regarding the potential effects of such intermolecular packing arrangements on the structure and function of nerve membranes. For example, one prediction might be that the close apposition of acyl chains would reduce the permeability of the membranes to low molecular weight, water-soluble solutes. Another might be that tight packing arrangements among PE and PS molecules in a monolayer would favor lateral phase separation in the plane of the membrane and affect interactions of the monolayer with proteins and other molecules that are located in, or are in close contact with, the lipid bilayer. These are clearly all possibilities that could be tested experimentally. 

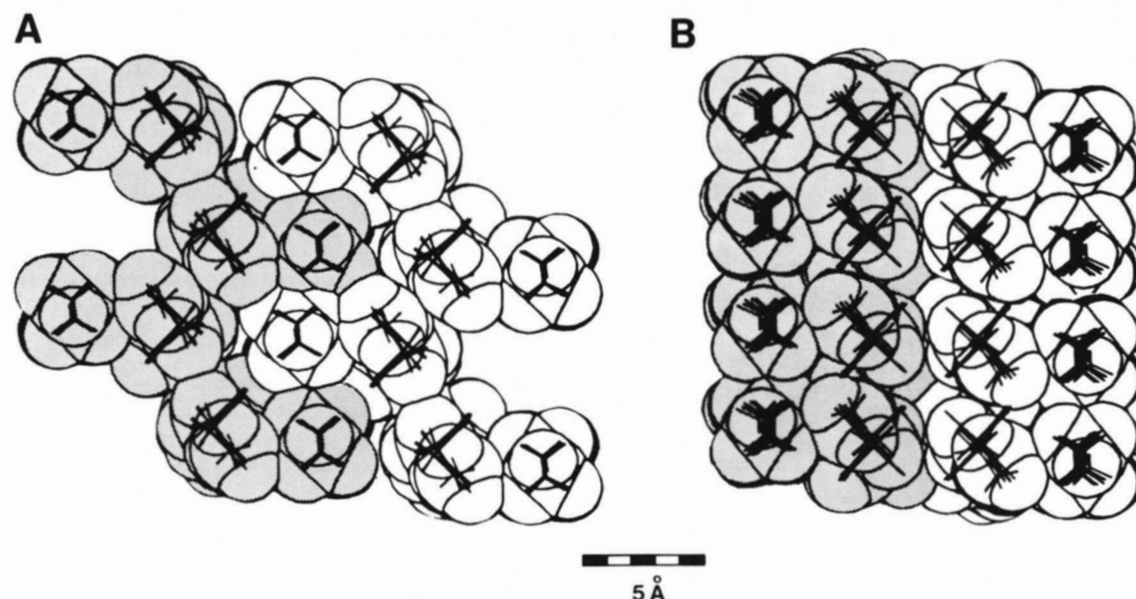


Fig. 16. Possible packings for acyl chains in a monolayer of 1-stearoyl-2-docosahexaenoyl PE molecules. Cross-sectional views of only the acyl chains are projected onto the plane of the monolayer. Although these arrays could not be refined to minimum energy conformations because of the limitations of the MM2 program (see Methods), MM2 minimum energy diacylglycerols were used to generate the cross sections and various minimum energy packings of hydrocarbon chains were used as a guide for arranging the molecules relative to one another. In each row of the arrays, saturated and hexanoic chains belonging to the same diacylglycerol molecule are shaded (left molecule) or unshaded (right molecule). A. A packing of PE molecules containing angle iron-shaped DHA chains. The various chain-chain interactions, saturated-saturated, saturated-polyunsaturated, and polyunsaturated-polyunsaturated, all have similar packing energies (see Table 4). This should produce a monolayer with rather homogeneous physical properties. B. A packing of PE molecules containing helical DHA chains. Only incomplete "edge-to-edge" contacts are possible between helices, while strong interactions can occur between saturated chains. This would be expected to produce an inhomogeneous distribution of packing energies and destabilize this arrangement relative to the one in part A.

APPENDIX

I. Relative orientation of double bonds in 1,4-pentadiene

We used the following approach to determine how the orientation of the two double bonds in 1,4-pentadiene varies as a function of the torsion angles for rotation about the central methylene carbon atom. Following the formalism of Go and Scheraga (35), we defined local Cartesian coordinate systems at carbon atoms 2, 3, and 4 (see Fig. 2). We defined rotation transformers and bond vectors of the forms

$$T_i = \begin{pmatrix} \cos \theta_i & -\sin \theta_i & 0 \\ \sin \theta_i & \cos \theta_i & 0 \\ 0 & 0 & 1 \end{pmatrix} \quad R_i = \begin{pmatrix} 1 & 0 & 0 \\ 0 & \cos \omega_i & -\sin \omega_i \\ 0 & \sin \omega_i & \cos \omega_i \end{pmatrix}$$

$$P_i = [d_i, 0, 0]$$

as functions of bond angle supplements θ_i , torsion angles ω_i , and bond lengths d_i , respectively. Then any vector r_4 in the coordinate system associated with the second double bond could be transformed to an equivalent vector r_2 in the coordinate system for the first double bond by the matrix equation

$$r_2 = T_2 \cdot R_3 \cdot T_3 \cdot R_4 \cdot r_4 + T_2 \cdot R_3 \cdot p_3 + p_2$$

The first term represents a rotation of the vector, while the other terms specify a translation which superimposes the origins of the coordinate systems. Only the first term needs to be considered for calculations of the angles of intersection between the double planes or between the bond direction vectors.

The orientation of the plane containing a double bond and its substituent atoms can be defined by a unit vector normal to the plane of the form $[0,0,1]$ in the local coordinate system. Such normal vectors n_2 and

n_4 can be defined for the two double bonds. Vector n_4 can be transformed to $n_4'' = T_2 \cdot R_3 \cdot T_3 \cdot R_4 \cdot n_4$ in the coordinate system for the first double bond. The dihedral angle between the two double-bond planes is then given by the dot product of the normal vectors as $\cos \alpha = n_2 \cdot n_4''$.

In similar fashion, unit vectors b_2 and b_3 (of the form $[1,0,0]$ in local coordinates) can be defined parallel to the double bonds. After the transformation $b_3'' = T_2 \cdot R_3 \cdot T_3 \cdot R_4 \cdot b_3$, the angle β between the double bond directions can be determined as $\cos \beta = b_2 \cdot b_3''$. If the matrices and vectors are multiplied explicitly, the resulting algebraic equations are:

$$\cos \alpha = \cos \omega_3 \cos \omega_4 - \cos \theta_3 \sin \omega_3 \sin \omega_4$$

$$\begin{aligned} \cos \beta = & \cos \theta_2 \cos \theta_3 \cos \theta_4 - \sin \theta_2 \sin \theta_3 \cos \theta_4 \cos \omega_3 \\ & - \cos \theta_2 \sin \theta_3 \sin \theta_4 \cos \omega_4 + \sin \theta_2 \sin \theta_4 \sin \omega_3 \sin \omega_4 \\ & - \sin \theta_2 \cos \theta_3 \sin \theta_4 \cos \omega_3 \cos \omega_4 \end{aligned}$$

These equations or the direct matrix transformation commands of PL/PROPHET (10, 11) generated identical numerical results, which were then used to construct the contour plot of Fig. 4.

II. Calculation of geometrically allowed torsion angle sequences for the bridge bonds between acyl chains in diacylglycerols

The acyl chains and part of the glycerol moiety of a diacylglycerol form a linear sequence of bonds. If the acyl chains are to be aligned parallel to one another, the bond angles and lengths of the intervening bonds set constraints on the allowed torsion angles for those bonds. Go and Scheraga (35) showed that the permitted sets of torsion angles may be calculated for sequences of six consecutive bonds connecting the fixed ends of a molecule. There may be multiple solutions, or no solutions at all, depending upon the exact relative orientation and separation of the fixed portions.

We implemented the Go and Scheraga equations as a PL/PROPHET program FINDTORSIONS, that took advantage of commands in the language to access molecular structures or carry out vector and matrix manipulations. The program included a robust algorithm for finding roots of nonlinear equations, which was translated from a published Fortran program (55). FINDTORSIONS searched automatically for all solution sets of torsion angles that were compatible with any given orientation of the fixed ends of the molecule.

Even though the FINDTORSIONS program determined geometrically permitted bridging structures between the acyl chains of a diacylglycerol, we found it necessary to use two additional criteria before accepting a conformation as a possibly valid physical structure that could be packed in a membrane. The conformation had to be free of large amounts of strain or steric hindrance and had to correspond to a local minimum of the steric energy surface. Furthermore, the hydrophilic free hydroxyl group had to be oriented away from the region of the hydrophobic acyl chains.

This investigation was supported by U.S. Public Health Service grant RR-00166 and by the Howard Hughes Medical Institute.

Manuscript received 18 November 1985.

REFERENCES

1. Mead, J. F., and A. J. Fulco. 1976. The Unsaturated and Polyunsaturated Fatty Acids in Health and Disease. Charles C. Thomas, Springfield, IL.
2. Breckenridge, W. C., G. Gombos, and I. G. Morgan. 1972. The lipid composition of adult rat brain synaptosomal plasma membranes. *Biochim. Biophys. Acta*. **266**: 695-707.
3. Dratz, E. A., and A. J. Deese. 1986. The role of docosahexaenoic acid in biological membranes: examples from photoreceptors and model membrane bilayers. In *Health Effects of Polyunsaturated Fatty Acids in Seafoods*. A. P. Simopoulos, R. R. Kiefer, and R. E. Martin, editors. Academic Press, New York. In press.
4. Darin-Bennett, A., A. Poulos, and I. G. White. 1976. The fatty acid composition of the major phosphoglycerides of ram and human spermatozoa. *Andrologia*. **8**: 37-45.
5. Phillips, G. B., and J. T. Dodge. 1967. Composition of phospholipids and of phospholipid fatty acids of human plasma. *J. Lipid Res.* **8**: 676-681.
6. Crawford, M. A., A. G. Hassam, G. Williams, and W. Whitehouse. 1977. Fetal accumulation of long-chain polyunsaturated fatty acids. *Adv. Exp. Med. Biol.* **83**: 135-143.
7. Neuringer, M., W. E. Conner, C. Van Petten, and L. Barstad. 1984. Dietary omega-3 fatty acid deficiency and visual loss in infant rhesus monkeys. *J. Clin. Invest.* **73**: 272-276.
8. Stubbs, C. D., and A. D. Smith. 1984. The modification of mammalian membrane polyunsaturated fatty acid composition in relation to membrane fluidity and function. *Biochim. Biophys. Acta*. **779**: 89-137.
9. Raub, W. F. 1974. The PROPHET system and resource sharing. *Federation Proc.* **33**: 2390-2392.
10. Rindone, W. P., and T. Kush. 1980. PROPHET Molecules. A User's Guide to the Molecule Facilities of the PROPHET System. Bolt, Beranek, and Newman, Inc., Cambridge, MA.
11. Wood, J. J. 1978. User's guide to PL/PROPHET. A Language Reference Manual for the PROPHET System. Bolt, Beranek, and Newman, Inc., Cambridge, MA.
12. Burkert, U., and N. L. Allinger. 1982. Molecular Mechanics. (ACS Monograph). 177. American Chemical Society, Washington, DC. 1-339.
13. Allinger, N. L. 1977. Conformational analysis. 130. MM2. A hydrocarbon force field utilizing V1 and V2 torsional terms. *J. Am. Chem. Soc.* **99**: 8127-8134.
14. Allinger, N. L., and Y. H. Yuh. 1980. Molecular Mechanics. Operating Instructions for MM2 and MMP2 Programs. QCPE 423. Quantum Chem. Program Exchange, Bloomington, IN. 1-87.
15. Prinz, H. 1983. The MM2/PROPHET Molecular Modeling System. Bolt, Beranek, and Newman, Inc., Cambridge, MA. 1-21.
16. Barry, D. 1985. Some Notes on Running the MM2P Molecular Mechanics Package in PROPHET. Bolt, Beranek, and Newman, Inc., Cambridge, MA. 1-10.
17. Sundaralingam, M. 1972. Molecular structures and conformations of the phospholipids and sphingomyelins. *Ann. N.Y. Acad. Sci.* **195**: 324-355.
18. Hauser, H., I. Pascher, R. H. Pearson, and S. Sundell. 1981. Preferred conformation and molecular packing of phosphatidylethanolamine and phosphatidylcholine. *Biochim. Biophys. Acta*. **650**: 21-51.
19. Gallinella, E., and B. Cadioli. 1975. Rotational isomerism and structure of penta-1,4-diene: raman spectrum and ab initio calculations. *J. Chem. Soc. Faraday II*: 781.
20. Meyer, E. J. 1983. CONTOUR. Bolt, Beranek, and Newman, Inc., Cambridge, MA. 1-5.
21. Rohrer, D. 1980. SPACEMOL. In *Prophet Molecules*. W. P. Rindone, and T. Kush, editors. Bolt, Beranek, and Newman, Inc., Cambridge, MA. 5-103-5-106.
22. Shimanouchi, T., Y. Abe, and Y. Alaki. 1971. Stable conformations of 1,4-polybutadiene chains and their model compounds. *Polymer J.* **2**: 199-211.
23. Kondo, S., E. Hirota, and Y. Morino. 1968. Microwave spectrum and rotational isomerism in butene-1. *J. Mol. Spectrosc.* **28**: 471-489.
24. Inagaki, F., M. Sakakibara, I. Harada, and T. Shimanouchi. 1975. Infrared and raman spectra and rotational isomerism of 1,4-pentadiene. *Bull. Chem. Soc. Japan*. **48**: 3557-3560.
25. Ernst, J., W. S. Sheldrick, and J. H. Fuhrhop. 1979. The structures of the essential unsaturated fatty acids, crystal structure of linoleic acid as well as evidence for the crystal structure of alpha-linolenic acid and arachidonic acid. *Z. Naturforsch.* **84b**: 701-711.
26. Abe, Y., and P. J. Flory. 1971. Configurational statistics of 1,4-polybutadiene chains. *Macromolecules*. **4**: 219-229.
27. Schurinck, W. T., and S. de Jong. 1977. Ab initio molecular orbital calculations on the conformations of some unsaturated fragments of lipid molecules: 1-butene, *cis*-2-pentene, and 1,4-pentadiene. *Chem. Phys. Lipids*. **19**: 313-322.
28. Salvetti, F., A. Buttinoni, R. Cesarani, and C. Tosi. 1981. Relationship between a hydrophobic cyclooxygenase site model and indoprofen structure. *Eur. J. Med. Chem.* **16**: 81-90.
29. Abrahamsson, S., and I. Ryderstedt-Nahringbauer. 1962. The crystal structure of the low-melting form of oleic acid. *Acta Crystallogr.* **15**: 1261.
30. Seelig, A., and J. Seelig. 1977. Effect of a single *cis* double bond on the structure of a phospholipid bilayer. *Biochemistry*. **16**: 45-50.
31. Seelig, J., and J. Waespe-Sarcevic. 1978. Molecular order in *cis* and *trans* unsaturated phospholipid bilayers. *Biochemistry*. **17**: 3310-3315.
32. Stubbs, C., T. Kouyama, K. Kinoshita, and A. Ikegami. 1981. Effect of double bonds on the dynamic properties of the hydrocarbon region of lecithin bilayers. *Biochemistry*. **20**: 2800-2810.
33. Small, D. M. 1984. Lateral chain packing in lipids and membranes. *J. Lipid Res.* **25**: 1490-1500.
34. Elder, M., P. Hitchcock, R. Mason, and G. G. Shipley.

1977. A refinement analysis of the crystallography of the phospholipid, 1,2-dilauroyl-DL-phosphatidylethanolamine, and some remarks on lipid-lipid and lipid-protein interactions. *Proc. R. Soc. Lond. A*. **354**: 157-170.
35. Go, N., and H. A. Scheraga. 1970. Ring closure and local conformational deformations of chain molecules. *Macromolecules*. **3**: 178-187.
36. Berde, C. B., H. C. Andersen, and B. S. Hudson. 1980. A theory of the effects of head-group structure and chain unsaturation on the chain melting transition of phospholipid dispersions. *Biochemistry*. **19**: 4279-4293.
37. Frischleder, H., R. Krahle, and E. Lehman. 1981. Intra- and intermolecular interactions of phospholipid headgroups within a two-dimensional hexagonal lattice. *Chem. Phys. Lipids*. **28**: 291-304.
38. Frischleder, H., and G. Peinel. 1982. Quantum-chemical and statistical calculations on phospholipids. *Chem. Phys. Lipids*. **30**: 121-158.
39. McAlister, J., N. Yathindra, and M. Sundaralingam. 1973. Potential energy calculations on phospholipids. Preferred conformations with intramolecular stacking and mutually tilted hydrocarbon chain planes. *Biochemistry*. **12**: 1189-1195.
40. Vanderkooi, G. 1973. Conformational analysis of phosphatides: mapping and minimization of the intramolecular energy. *Chem. Phys. Lipids*. **11**: 148-170.
41. Marcelja, S. 1974. Chain ordering in liquid crystals. II. Structure of bilayer membranes. *Biochim. Biophys. Acta*. **367**: 165-176.
42. Gruen, D. W. R. 1982. Statistical thermodynamics of alkyl chain conformations in lipid bilayers. *Chem. Phys. Lipids*. **30**: 105-120.
43. Gruen, D. W. R. 1980. A statistical mechanical model of the lipid bilayer above its phase transition. *Biochim. Biophys. Acta*. **595**: 161-183.
44. Brasseur, R., E. Goormaghtigh, and J. M. Ruysschaert. 1981. Theoretical conformational analysis of phospholipid bilayers. *Biochem. Biophys. Res. Commun.* **103**: 301-310.
45. Brosio, E., F. Conti, and A. Di Nola. 1977. A stereochemical model for phospholipids. I. Conformational energy refinement and molecular packing of L-alpha-dipalmitoyl-lecithin (DPL). *J. Theor. Biol.* **67**: 319-334.
46. Peinel, G., H. Frischleder, and H. Binder. 1983. Quantum-chemical and empirical calculations on phospholipids. VIII. The electrostatic potential from isolated molecules up to layer systems. *Chem. Phys. Lipids*. **33**: 195-205.
47. Nakagawa, Y., and L. A. Horrocks. 1983. Separation of alkenylacyl, alkylacyl, and diacyl analogues and their molecular species by high performance liquid chromatography. *J. Lipid Res.* **24**: 1268-1275.
48. Dekker, C. J., W. S. Geurts Van Kessel, J. P. G. Klomp, J. Pieters, and B. De Kruijff. 1983. Synthesis and polymorphic phase behavior of polyunsaturated phosphatidylcholines and phosphatidylethanolamines. *Chem. Phys. Lipids*. **33**: 93-106.
49. Ghosh, D., M. A. Williams, and J. Tinoco. 1973. The influence of lecithin structure on their monolayer behavior and interactions with cholesterol. *Biochim. Biophys. Acta*. **291**: 351-362.
50. Demel, R. A., W. S. Geurts Van Kessel, and L. L. M. VanDeenen. 1972. The properties of polyunsaturated lecithins in monolayers and liposomes and the interactions of these lecithins with cholesterol. *Biochim. Biophys. Acta*. **266**: 26-40.
51. Deese, A. J., E. A. Dratz, F. W. Dahlquist, and M. R. Paddy. 1981. Interaction of rhodopsin with two unsaturated phosphatidylcholines: a nuclear magnetic resonance study. *Biochemistry*. **20**: 6420-6427.
52. Coolbear, K. P., C. B. Berde, and K. M. W. Keough. 1983. Gel to liquid-crystalline phase transition of aqueous dispersions of polyunsaturated mixed-acid phosphatidylcholines. *Biochemistry*. **22**: 1466-1473.
53. Paddy, M. R., F. W. Dahlquist, E. A. Dratz, and A. J. Deese. 1985. Simultaneous observation of order and dynamics at several defined positions in single acyl chain using ^2H NMR of single acyl chain perdeuterated phosphatidylcholines. *Biochemistry*. **24**: 5988-5995.
54. Fukushima, E., and S. B. W. Roeder. 1981. *Experimental Pulse NMR: A Nuts and Bolts Approach*. Addison-Wesley, Reading, MA.
55. Shampine, L. F., and R. C. Allen. 1973. *Numerical Computing: An Introduction*. W. B. Saunders Co., Philadelphia. 242-246.
56. Cambridge Crystallographic Database. *Practical Guide to Search, Retrieval, Analysis, and Display*. 1981. Cambridge Crystallography Data Centre, Cambridge, England. 1-91.